

Can Flavor Physics Hint at Distinctive Signals for R-parity Violation at the LHC?

Biplob Bhattacharjee ^{a,1}, Gautam Bhattacharyya ^{b,2}, and Sreerup Raychaudhuri ^{a,3}

^{a)} Department of Theoretical Physics, Tata Institute of Fundamental Research,
1 Homi Bhabha Road, Mumbai 400 005, India.

^{b)} Saha Institute of Nuclear Physics, 1/AF Bidhan Nagar, Kolkata 700 064, India.

ABSTRACT

Observation of some low-energy processes in the flavor physics regime may require the existence of supersymmetry with two relatively large R-parity-violating couplings of the LQD-type, together with reasonably light superparticles. At the LHC, such interactions would be expected to give rise to clear signals with convenient leptonic triggers, including some multileptons of the same sign. We undertake a detailed investigation of these signals taking care to correlate with low-energy requirements and taking proper account of the Standard Model backgrounds as well as the R-parity-conserving sector of the supersymmetric model. We find clear indications that R-parity violation as envisaged in this scenario can be detected at the LHC — even, perhaps, in the early runs.

PACS numbers: 11.30.14v, 14.20.Sv, 12.60.Jv

November 16, 2017

¹biplob@theory.tifr.res.in

²gautam.bhattacharyya@saha.ac.in

³sreerup@theory.tifr.res.in

1 Introduction: Unifying Approaches

The Standard Model (SM), which represents the culmination of eighty years of investigation into the nature and properties of elementary particles, can be described as both a triumph and a tragedy. The triumph lies in our having been able to put together a stable, working model which explains a whole world of empirical data to an accuracy which sometimes reaches the amazing value of one in a hundred thousand. The tragedy is that the selfsame model is really a portmanteau containing disparate, not-so-compatible theoretical ideas and a bunch of purely phenomenological parameters, and hence, lacks credibility as a final theory. Normally, such an obviously-incomplete theory would be expected to fall apart under the impact of systematic empirical study, but the SM seems to have passed four decades of stringent experimental testing with flying colors [1]. Much debate and discussion [2] during this period has made it quite clear that if we are to bridge some of these gaps in our understanding, we must invoke new physics beyond the SM, even though all efforts to find empirical evidence for such new physics have so far proved futile. It is, therefore, vital to the progress of the subject that we continue our search for new physics in all possible ways. Moreover, the lesson to be learnt from the failure of previous searches is that the task at hand is by no means an easy one and hence, we should bring all possible resources to bear upon the problem.

In this all-encompassing pursuit of new physics beyond the SM, the bulk of terrestrial experimentation is being channelled, at the present juncture of time, along two more-or-less parallel approaches. One is the set of low-energy experiments probing flavor physics in meson production and decay modes, such as the BELLE, BaBar and Fermilab Tevatron experiments, where one hopes that as more and more statistics is gathered, some unusual flavor-changing processes might be observed at rates larger than predicted in the SM. To this category also belong the different neutrino experiments probing flavor violation in the leptonic sector. The other approach is that of running accelerators at the high energy frontier, specifically at CERN's Large Hadron Collider (LHC), where the general hope is that new particles may begin to make their appearance as the centre-of-mass energy and the luminosity of this machine are pushed to hitherto-unattained levels. The former approach is sensitive to new physics through virtual effects, i.e. they work because of quantum mechanics. Such effects would provide only indirect clues, of course, but they have the advantage of not being restricted by the machine energy. The latter approach can confirm the existence of new physics by direct creation and detection of heavy, unstable particles, i.e. this approach works because of special relativity. Direct discovery is, of course, the best kind of existence proof, but in this case it is severely constrained by the kinematic reach of the LHC machine. We thus have two experimental paradigms — one looking for virtual states and one for real states. However, just as quantum mechanics and special relativity are not mutually incompatible, neither are the above approaches mutually exclusive, and they do not need to be pursued in isolation. What seems to be called for is a dexterous amalgamation of the two different techniques, one providing hints of the nature of couplings and masses of the new physics and the other following those leads in order to pin it down completely. More specifically, if there is a model of new physics which contributes to

low energy processes at levels which would soon become testable, it is imperative to check out the possible signals of such a model at the LHC; conversely, if a model seems accessible to detection at the LHC, one would immediately ask what its low-energy consequences are. This article builds on such an idea and makes a naive – but nonetheless robust – attempt at unifying the two approaches.

To be more specific, in this work we consider a model of R-parity-violating (RPV) supersymmetry [3] and study its dual impact, viz., on the one hand, its influence in flavor physics through virtual effects, and on the other, its prediction of specific multilepton and jet final states at the LHC leading to possible identification of superparticle resonances. As is well known, R-parity is a discrete symmetry defined by $\mathcal{R} = (-)^{3\mathcal{B}+\mathcal{L}+2\mathcal{S}}$, where \mathcal{B} , \mathcal{L} , and \mathcal{S} are, respectively, the baryon number, lepton number and spin of a particle: thus we have $\mathcal{R} = +1$ for all SM particles, while $\mathcal{R} = -1$ for their superpartners. We begin by noting that conservation of R-parity, though a popular ingredient in models of supersymmetry, is not demanded by any deep underlying principle. It was originally introduced by Farrar and Fayet [3] to prevent fast proton decay through operators which violate lepton and baryon number. However, it was later pointed out by Weinberg and others [3] that it is phenomenologically sufficient to conserve baryon number but not lepton number, or vice versa, in order to ensure stability of the proton. Most supersymmetric grand unified theories prefer a ‘baryon parity’ which calls for baryon number conservation, because this is anomaly-free [4], and hence, most of the literature on RPV tends to violate lepton number through either $LL\bar{E}$ or $LQ\bar{D}$ operators. Baryon number conservation is, therefore, taken implicitly in our work. We then go on to argue, following Ref. [5], that the simultaneous presence of some specific RPV operators in the superpotential can provide correlated enhancements over the SM prediction in several flavor-changing neutral current (FCNC) channels and thereby predict flavor-changing leptonic decays at experimentally-verifiable levels which lie far above the SM expectations. Fixing the parameters of this model to the values demanded by this requirement, we then go on to study the impact of such interactions in superparticle production and decays at the LHC. It turns out that with these assumptions distinctive and rather spectacular signals are predicted for a wide range of parameters in the R-parity-conserving (RPC) sector of the model. The techniques used in our analysis, though applied in the context of specific RPV couplings as above, are fairly general and can be easily adapted to search for any RPV signal due to operators of the same type. There is a pleasing synergy, therefore, between flavor physics studies such as those of Ref. [5] and our LHC study, viz., discovery of some of the FCNC effects predicted at low energies would imply spectacular signals at the LHC and discovery of some such signals at the LHC would immediately tell us that some spectacular FCNC effects must occur at low energies.

Our work differs from previous collider studies for RPV [6] in that we do not allow the masses and couplings relevant to the RPV sector to vary freely and independently (as has been done by previous workers in the field), but constrain them by the requirement that they should predict a certain set of low-energy FCNC effects at or close to their present upper bounds. In a sense it is this *assumption* which directly leads to correlation of large new physics signals in low-energy processes with spectacular LHC signals, and vice versa. It is also worth pointing out that some

of the signals for RPV at the LHC do not depend very crucially on this correlation of couplings – thus, these would be observed even if we do not invoke any low-energy connection.

The plan of the article is as follows. In the next section, we summarize the arguments set out in detail in Ref. [5], explaining the requirement for specific terms in the superpotential. We then discuss the different possibilities for non-SM LHC signals which are thrown up by the presence of these operators in Section 3. Section 4 is devoted to the study of resonances in these non-SM signals, while Section 5 discusses the case when resonances would not be apparent. Section 6 discusses same-sign leptons and the discovery limits using these signals. In the concluding Section 7 we include a critical summary of our results.

2 R-Parity Violation: the Flavor Connection

The fact that large mixing of neutrino flavors (*maximal* mixing between ν_μ and ν_τ) has been firmly established [7] has set afoot speculations that lepton flavor-violating (LFV) transitions could also be observed in the charged lepton sector. However, if this were to proceed in exact analogy with the quark sector, then the unitarity of the mixing matrix and the smallness of the neutrino masses would jointly ensure that SM predictions for LFV decays of charged leptons ℓ_i ($= e, \mu, \tau$) would lie far below any detectable level¹. It follows that actual observation of processes like, e.g.,

$$\ell \rightarrow 3 \ell' , \quad \ell \rightarrow \ell' + \gamma , \quad \ell \rightarrow \ell' + P ,$$

where P is a pseudoscalar meson and ℓ and ℓ' are leptons of different flavour, would immediately and unambiguously establish the existence of new physics beyond the SM. These are expected to be probed with ever-increasing sensitivity in different ongoing and upcoming experiments [8]. Concerning such new physics, two comments are in order, viz.

- The new interaction(s) should be capable of enhancing the LFV decay rates, but at the same time keeping the light neutrino masses² under control, and
- If the above decays are observed near their present upper limits, then new physics at the tree level must be mediated by particles with weak scale couplings and having masses not more than a few hundred GeV.

Clearly, particles of this nature would be copiously produced at the LHC. Moreover, differential rates of LFV decays could be directly linked to the relative abundance of one lepton flavor over another in observed final states at the LHC and therefore, provide prior motivation for choosing preferential lepton triggers in the detection process.

¹This is analogous to the Glashow-Iliopoulos-Maiani (GIM) cancellation in the quark sector, except that the residual effects are much smaller, being suppressed by the tiny neutrino masses.

²Generation of Majorana masses, of course, requires lepton number violation by two units.

In this paper, we concentrate on the \mathbb{L} -violating λ' -type superpotential, given in terms of chiral superfields, by

$$\widehat{W} = \sum_{i,j,k=1}^3 \lambda'_{ijk} \left(\widehat{\nu}_{Li} \widehat{d}_{Lj} - \widehat{\ell}_{Li} \widehat{u}_{Lj} \right) \widehat{d}_{Rk}^c \quad (1)$$

where i, j, k are generation indices. These lead to LFV interactions whose strength is determined by the 27 coupling constants λ'_{ijk} . Phenomenological constraints exist on each of these λ'_{ijk} couplings and also on many of their products, taken pairwise [9, 10]. However, if we consider all 27 of them together the phenomenological situation would become chaotic and it would be well-nigh impossible to make definite predictions. It is usual, therefore, to work with a small number – often just one – of the λ'_{ijk} couplings, which are assumed to be large, while the others are zero or vanishingly small. This kind of scenario is inspired by the structure of Yukawa couplings in the SM, which are large only in the third generation, while the others are negligibly small by comparison. In this work, we select only two of the λ'_{ijk} couplings, namely λ'_{223} and λ'_{323} to be large, i.e., close to their present upper limits.

The question immediately arises: why choose just this pair of third-generation couplings λ'_{223} and λ'_{323} to be large, when there are many possible choices? Before justifying our choice, however, let us review the existing constraints on these two couplings. Limits from low-energy processes will always depend on the mass \tilde{m} of the \tilde{c}_L scalar, or the \tilde{b}_R scalar. Keeping in mind the present direct search limit on squarks from their non-observation from the Tevatron experiment [7], we assume a benchmark sparticle mass $\tilde{m} = 300$ GeV for this part of our analysis. Then, the best upper limit on λ'_{223} comes from [9, 10, 11]

$$R_{D^0} \equiv \frac{\text{BR}(D^0 \rightarrow K^- \mu^+ \nu_\mu)}{\text{BR}(D^0 \rightarrow K^- e^+ \nu_e)},$$

and its value is

$$\lambda'_{223} \lesssim 0.3 \left(\frac{\tilde{m}}{300 \text{ GeV}} \right) \quad (2)$$

at 90% C.L.. On the other hand, the best upper limit on λ'_{323} arises from [10]

$$R_{D_s}(\tau\mu) \equiv \frac{\text{BR}(D_s^+ \rightarrow \tau^+ \nu_\tau)}{\text{BR}(D_s^+ \rightarrow \mu^+ \nu_\mu)},$$

and the 90% C.L.value is

$$\lambda'_{323} \lesssim 0.9 \left(\frac{\tilde{m}}{300 \text{ GeV}} \right) \quad (3)$$

These upper bounds of 0.3 and 0.9 respectively (for $\tilde{m} = 300$ GeV) are rather high and comparable to the values of the electroweak couplings. However, as the mass $\tilde{m} = 300$ GeV is significantly higher than the masses of the electroweak gauge bosons, the RPV effects would be weaker than SM effects of the same order. In fact, these new physics effects can only dominate processes where the same-order SM effects are suppressed, e.g. by a GIM-type mechanism.

We now come to the special role played by λ'_{223} and λ'_{323} . It turns out [5] that the joint action of these two couplings can trigger a variety of potentially-observable phenomena, such as those listed below.

- Generation of neutrino masses: Quite generally, neutrino mass terms are generated at the one-loop level via λ' couplings by combinations $\lambda'_{ijk}\lambda'_{i'kj}$, which yield $[m_\nu]_{ii'}$. Typically, for a sfermion mass of 300 GeV, these products of coupling constants will have an upper limit of 10^{-4} to 10^{-6} [12], where the exact limit depends on the mass of the fermions of the j and k generations. However, if we take λ'_{223} and λ'_{323} as the only large (~ 0.5) couplings (together with a small $\lambda'_{113} \lesssim 0.1$), neutrino masses are not generated at one loop, but an acceptable pattern of elements in the neutrino mass matrix emerges at the two-loop level [13]. The key point here is that it is essentially the two-loop suppression factor that allows λ'_{223} and λ'_{323} to be as large as their upper limits obtained from other phenomenological considerations, provided all the other λ' couplings are small.
- Higher rates for LFV decays: The simultaneous presence of couplings λ'_{223} and λ'_{323} induces LFV decays of the τ lepton, viz.

$$\tau \rightarrow 3\mu, \quad \tau \rightarrow \mu\gamma, \quad \tau \rightarrow \mu\eta, \quad \tau \rightarrow \mu\eta',$$

at numerically significant rates. The scalars that mediate these processes are \tilde{b}_R and \tilde{c}_L . As before, we denote the mass of a generic scalar by \tilde{m} . We also define a ‘product coupling’ $\lambda' \equiv \sqrt{\lambda'_{223}\lambda'_{323}}$. The numerical contributions to different branching ratios and their dependence on λ' and \tilde{m} are given by [5]:

$$\begin{aligned} \text{BR}(\tau \rightarrow 3\mu) &\simeq 3.9 \times 10^{-7} \left[1.0 - 0.6 \left(\frac{\lambda'}{0.7} \right)^2 + 0.1 \left(\frac{\lambda'}{0.7} \right)^4 \right] \left(\frac{\lambda'}{0.7} \right)^4 \left(\frac{300 \text{ GeV}}{\tilde{m}} \right)^4; \\ \text{BR}(\tau \rightarrow \mu\gamma) &\simeq 1.0 \times 10^{-6} \left(\frac{\lambda'}{0.7} \right)^4 \left(\frac{300 \text{ GeV}}{\tilde{m}} \right)^4; \\ \text{BR}(\tau \rightarrow \mu\eta) &\simeq 3.4 \times 10^{-7} \left(\frac{\lambda'}{0.7} \right)^8 \left(\frac{300 \text{ GeV}}{\tilde{m}} \right)^4; \\ \text{BR}(\tau \rightarrow \mu\eta') &\simeq 3.3 \times 10^{-7} \left(\frac{\lambda'}{0.7} \right)^8 \left(\frac{300 \text{ GeV}}{\tilde{m}} \right)^4. \end{aligned} \quad (4)$$

These may be compared with the present experimental upper limits of the above branching ratios, as listed by the Particle Data Group [7], which are

$$\begin{aligned} \text{BR}(\tau \rightarrow \mu^- \mu^+ \mu^-) &< 3.2 \times 10^{-8}, \\ \text{BR}(\tau \rightarrow \mu^- \gamma) &< 4.5 \times 10^{-8}, \\ \text{BR}(\tau \rightarrow \mu^- \eta) &< 6.5 \times 10^{-8}, \\ \text{and } \text{BR}(\tau \rightarrow \mu^- \eta') &< 1.3 \times 10^{-7}. \end{aligned} \quad (5)$$

It is clear that these upper limits can easily be saturated by quite reasonable values of λ' , for $\tilde{m} = 300$ GeV. Eq. (4) also indicates that the upper bound on λ' scales linearly with \tilde{m} .

It is expected [8] that the SuperB factory with 75 ab^{-1} luminosity will probe the branching ratios of the $\tau^- \rightarrow \mu^- \mu^- \mu^+$ and $\tau^- \rightarrow \mu^- \eta$ to the level of 2×10^{-10} and 4×10^{-10} respectively. There exists the exciting possibility that these LFV processes would be seen in such

experiments, vindicating the hypothesis of RPV; on the other hand, negative results would place stringent bounds on the product coupling λ' . At present, however, the best limit on the product coupling λ' arises from $\text{BR}(\tau \rightarrow \mu\gamma)$, and is given at 90% C.L. by

$$\lambda' \lesssim 0.3 \left(\frac{\tilde{m}}{300 \text{ GeV}} \right). \quad (6)$$

This is comparable with the individual bounds on λ'_{223} and λ'_{323} mentioned above.

- *CP violation in the B_s - \bar{B}_s system*: A very small, but nonvanishing, λ'_{212} (~ 0.001), together with a large λ'_{223} (~ 0.5), can generate a large phase in B_s - \bar{B}_s mixing [14].
- *Leptonic decays of the D_s meson*: The product coupling λ' can also contribute [15] at the tree level to the rare decays $D_s \rightarrow \ell\nu$ ($\ell \equiv \mu, \tau$). At the quark level, the process corresponds to $c \rightarrow s\ell\nu$. It follows, therefore, that the SM branching ratio would be proportional to $G_F^2 |V_{cs}|^2 f_{D_s}^2$. Once the RPV couplings are turned on, the SM formula for the branching ratio in the $D_s \rightarrow \mu\nu$ channel is modified by replacing

$$G_F^2 |V_{cs}|^2 \longrightarrow \left| G_F V_{cs}^* + \frac{\lambda'_{223}}{4\sqrt{2}\tilde{m}^2} \right|^2 + \left| \frac{\lambda'_{223}\lambda'_{323}^*}{4\sqrt{2}\tilde{m}^2} \right|^2. \quad (7)$$

For $D_s \rightarrow \tau\nu$, we just need to replace $\lambda'_{223} \leftrightarrow \lambda'_{323}$ in Eq. (7). We recall at this stage that Monte-Carlo simulations of QCD on the lattice [16] predict $f_{D_s} = 241 \pm 3$ MeV (HPQCD + UKQCD) and $f_{D_s} = 260 \pm 10$ MeV (FNAL + MILC + HPQCD). The experimental global average was initially $f_{D_s} = 277 \pm 9$ MeV [7, 17, 18]. It has now reduced somewhat, viz., $f_{D_s} = 257.5 \pm 6.1$ MeV [16], primarily due to the updated CLEO result [19].

A few comments regarding this process are in order. An earlier discrepancy between the first lattice result with smaller error bars and the initial experimental average had fuelled considerable speculation about the possible role of RPV [15] or leptoquark interactions [20] in the $D_s \rightarrow \ell\nu$ channel. It was shown [5], however, that the value of $\lambda' (\equiv \sqrt{\lambda'_{223}^* \lambda'_{323}}) > 0.3$ for $\tilde{m} = 300$ GeV required to explain the $D_s \rightarrow \ell\nu$ ‘anomaly’ was too large to be consistent with the upper bound $\lambda' < 0.3$ from $\text{Br}(\tau \rightarrow \mu\gamma)$. This tension has now disappeared as a result of the new experimental average mentioned above, and at present there is no urgency to invoke new physics at all in this channel. Nevertheless, the RPV couplings λ'_{223} and λ'_{323} do stand as potential contributors to this mode in case future measurements again create a divide between the SM prediction and the experimental result.

Apart from these cases, where the λ'_{223} and λ'_{323} couplings can possibly generate observable results which differ from the SM, one must take into account the possibility that these RPV couplings may be constrained by measurements of the anomalous magnetic moment of the muon. The maximum possible new physics contribution to this, parametrized as $a_\mu \equiv (g_\mu - 2)/2$, is estimated [21] as

$$a_\mu^{\text{new}} = a_\mu^{\text{exp}} - a_\mu^{\text{SM}} = (24.6 \pm 8.0) \times 10^{-10}. \quad (8)$$

In this case, the relevant coupling is λ'_{223} , and the induced contribution is given [5] by

$$a_{\mu}^{\text{RPV}} \simeq 1.9 \times 10^{-10} \left(\frac{\lambda'_{223}}{0.7} \right)^2 \left(\frac{300 \text{ GeV}}{\tilde{m}} \right)^2. \quad (9)$$

Clearly, even if we set $\lambda'_{223} \simeq 1$ in Eq. (9), we cannot saturate a_{μ}^{new} . This means that the present data on the muon anomalous magnetic moment pose no threat to having $\lambda' \sim 0.3$ with $\tilde{m} \simeq 300 \text{ GeV}$.

All in all, with two dominant (~ 0.5) couplings λ'_{223} and λ'_{323} , together with two significantly smaller and optional ones ($\lambda'_{212} \sim 0.001$ for two-loop neutrino mass generation and $\lambda'_{113} < 0.1$ for B_s - \bar{B}_s mixing), we can correlate several phenomena, real or projected, viz., LFV τ decays, generation of neutrino masses and mixing, leptonic D_s decays, and generation of a large phase in B_s mixing, without running afoul of constraints from the anomalous magnetic moment of the muon. We emphasize that no other viable form of new physics, including the very-similar leptoquark interactions, can correlate so many widely-disparate channels as our economical choice of only two dominant RPV couplings. With this as our motivation, we now turn to the issue of direct searches and seek to identify strategies to pinpoint supersymmetric interactions induced by these two couplings in the LHC environment.

3 Predicting Distinctive Signals at the LHC

In order to look for a viable process at a hadron collider like the LHC, we must take into account the fact that the best kind of signal requires a lepton tag and a reasonably large production cross-section. Ideally, the new particle production should involve strong interactions to give the large production cross-section and its decay should be to a leptonic or semi-leptonic channel to provide a good tag. The obvious candidate for such a signal is a *leptoquark*, i.e. a particle which carries both color and lepton number, for it can be produced through QCD processes and will inevitably decay into final states containing leptons. As is well known, the squarks of an RPV model behave as scalar leptoquarks, and hence will be equally good candidates for detection through leptonic tags.

Leptonic tags are also possible if the new particles carry a quantum number, conserved in strong interactions, which permits pair production of heavy particles, but disallows individual particles from decaying through strong interactions. This is possible in SUSY, where R parity plays the role of the conserved quantum number and the squarks and gluinos are produced through their strong interactions at the parton level. In the traditional RPC version of SUSY, these squarks and gluinos would then decay through cascades to quarks, W and Z bosons and eventually to the lightest supersymmetric particle (LSP) [22]. As is well known, in these models, the LSP is stable and is expected to lead to large amounts of missing transverse energy (MET) at a collider such as the LHC. This, combined with leptonic tags arising from decays of the W and/or the Z , produces the trilepton (four leptons) plus jets and MET signals which have traditionally been considered [23]

the most characteristic signatures of SUSY³.

The previous section has indicated the possibility that having observable low-energy signals may demand reasonably large values of two of the possible 45 RPV couplings, viz., λ'_{223} and λ'_{323} . This will lead [25] to the following interaction vertices:

$$\begin{aligned}\lambda'_{223} : \quad & \tilde{\nu}_\mu - s - b, \quad \tilde{s}_L - \nu_\mu - b, \quad \tilde{b}_R - \nu_\mu - s, \quad \tilde{\mu}_L - c - b, \quad \tilde{c}_L - \mu - b, \quad \tilde{b}_R - \mu - c \\ \lambda'_{323} : \quad & \tilde{\nu}_\tau - s - b, \quad \tilde{s}_L - \nu_\tau - b, \quad \tilde{b}_R - \nu_\tau - s, \quad \tilde{\tau}_L - c - b, \quad \tilde{c}_L - \tau - b, \quad \tilde{b}_R - \tau - c\end{aligned}$$

We now discuss the consequences of having these extra vertices at a collider like the LHC, especially the generation of novel processes leading to distinctive final states. As R parity remains conserved in the gauge sector of the model, the production cross-sections of squarks and gluinos will be unchanged. However, the squarks produced either directly, or from the decay of a gluino, would now have a competing channel to decay directly to a quark and a μ^\pm or τ^\pm (or to the corresponding neutrinos) through the RPV couplings λ'_{223} or λ'_{323} respectively. This is, in fact, the only channel available if the SM is extended by just a leptoquark, rather than the full spectrum of RPV supersymmetry. A glance at the vertices listed above will show that the most striking processes of this form are

$$p + p \xrightarrow{\mathcal{R}} \tilde{c}_L \tilde{c}_L^* \rightarrow (\mu^+ b)(\mu^- \bar{b}) \quad p + p \rightarrow \tilde{b}_R \rightarrow \tilde{b}_R^* \xrightarrow{\mathcal{R}} (\mu^- c)(\mu^+ \bar{c}) \quad (10)$$

and, likewise,

$$p + p \rightarrow \tilde{c}_L \tilde{c}_L^* \xrightarrow{\mathcal{R}} (\tau^+ b)(\tau^- \bar{b}) \quad p + p \rightarrow \tilde{b}_R \tilde{b}_R^* \xrightarrow{\mathcal{R}} (\tau^- c)(\tau^+ \bar{c}) \quad (11)$$

The symbol $(\xrightarrow{\mathcal{R}})$ indicates an R parity-violating decay. Clearly, a reconstruction of the invariant mass of the relevant $(\mu^\pm + b\text{-jet})$ or $(\tau^\pm + b\text{-jet})$ will show a resonant peak at the mass of the \tilde{c}_L squark and, likewise, the invariant mass of the $(\mu^\pm + c\text{-jet})$ or $(\tau^\pm + c\text{-jet})$ will peak at the mass of the \tilde{b}_R squark. Of these final states, the ones containing muons are the most viable since muons are somewhat easier to tag than τ jets in the messy hadronic environment of the LHC. Since this work is of exploratory nature, we focus on final states with a muon pair accompanied by a pair of hard jets – with the option of tagging the b -jets if required – and of course, with some level of fluctuation in jet number due to the usual phenomena of gluon radiation, fragmentation and merging of close jets. This is not to say that the signals with τ leptons are to be discounted, for they form a genuine check of the model in question, as well as being intrinsically detectable⁴. However, the signatures and detection strategies for τ signals will be rather similar to those for the muonic signals, except for somewhat lower efficiencies and slightly higher backgrounds arising from mistagging of QCD jets as τ 's. Since this work is of exploratory nature, we focus on the muonic signals and do not consider the τ signals any further. This also means that we discuss signals arising only from the R parity-violating coupling λ'_{223} .

³For alternative sources of such signals at the LHC, detailed discussions may be found in Ref. [24].

⁴Especially in view of improved tau-detection efficiencies claimed recently [26].

We have already noted that a squark \tilde{c}_L or \tilde{b}_R with R parity-violating couplings closely resembles a scalar leptoquark with similar couplings [27]. Had the only new physics component in question consisted of such leptoquarks, then we would need to go no further in discussing LHC signals, since these leptoquarks would decay solely (i.e. with branching ratio unity) to $\mu + b$ or $\tau + c$ final states. It will then be almost certain, as we shall demonstrate in the next section, that leptoquark resonances, if they exist and are kinematically accessible, will be seen in the 14 TeV run of the LHC.

The situation becomes more complicated — but also more interesting! — if we consider R parity-violating SUSY, instead of a simplistic leptoquark extension of the SM. For then, we also need to take into account the entire sparticle spectrum in addition to the squark \tilde{c}_L and \tilde{b}_R , together with their production modes and decay channels. Chief among these possibilities is that of production and decay of gluinos, which are strongly interacting and will be produced in numbers comparable to the squarks. One must also consider the charginos and neutralinos, which will couple to the squarks through their electroweak gauge couplings and provide competing decay channels to the leptoquark-like R parity-violating channels listed above. We must also take note of the fact that the gluinos and neutralinos are Majorana fermions, and hence can decay into final states with a μ^+ or a μ^- with equal probability — this gives rise to the possibility of same-sign multilepton states which are almost never found in the SM. Thus, R parity-violating SUSY permits more exotic signatures than are vouchsafed by the mere addition of a leptoquark to the SM.

In RPV supersymmetry, as envisaged here, there are two main scenarios, depending on the mass of the gluino \tilde{g} . If the gluino \tilde{g} happens to be heavier than the \tilde{c}_L (and \tilde{b}_R), then, in addition to the direct production of \tilde{c}_L (and \tilde{b}_R), these squarks can also arise from the cascade decays of gluinos (\tilde{g}), which would be pair produced at the LHC. We would then obtain substantial muon-rich events from hard processes of the form

$$\begin{aligned}
p + p \rightarrow \tilde{g} \tilde{g} \rightarrow (\bar{c} \tilde{c}_L)(\bar{c} \tilde{c}_L) \xrightarrow{\mathcal{R}} \bar{c} \bar{c} (\mu^+ b)(\mu^+ b) \quad ; \quad p + p \rightarrow \tilde{g} \tilde{g} \rightarrow (\bar{c} \tilde{c}_L)(c \tilde{c}_L^*) \xrightarrow{\mathcal{R}} c \bar{c} (\mu^+ b)(\mu^- \bar{b}) \\
p + p \rightarrow \tilde{g} \tilde{g} \rightarrow (c \tilde{c}_L^*)(\bar{c} \tilde{c}_L) \xrightarrow{\mathcal{R}} c \bar{c} (\mu^- \bar{b})(\mu^+ b) \quad ; \quad p + p \rightarrow \tilde{g} \tilde{g} \rightarrow (c \tilde{c}_L^*)(c \tilde{c}_L^*) \xrightarrow{\mathcal{R}} c c (\mu^- \bar{b})(\mu^- \bar{b})
\end{aligned}
\tag{12}$$

i.e. final states with a muon pair of like or unlike sign, typically accompanied by *four* hard jets, subject to jet-merging and other strong interaction effects, as listed above. Gluinos, being Majorana fermions, can decay with equal probability into \tilde{c}_L or \tilde{c}_L^* states, which accounts for the like- and unlike-sign muons in the final state. To every process listed above, there corresponds a similar process with the \tilde{b}_R squarks: these are not listed in the interests of brevity.

If, on the other hand, the gluino is lighter than the \tilde{c}_L and \tilde{b}_R , these squarks will tend to decay dominantly through the strong interaction to $\tilde{c}_L \rightarrow \tilde{g} + c$ and $\tilde{b}_R \rightarrow \tilde{g} + b$. The competing RPV decays will be suppressed, and hence, we will get a somewhat smaller multi-lepton signal of the form envisaged above. However, we note that the desire to have observable flavor physics effects

prompts us to take

$$\lambda'_{223} \simeq 0.3 \left(\frac{M(\tilde{c}_L)}{300 \text{ GeV}} \right) = \frac{M(\tilde{c}_L)}{1 \text{ TeV}} \quad (13)$$

for slightly larger values of $M(\tilde{c}_L)$. Thus, the branching ratio controlled by λ'_{223} grows larger for heavy \tilde{c}_L , and can remain substantial even when the gluino is lighter than the \tilde{c}_L . This is illustrated in Figure 1 for both the cases – where the gluino is lighter than the \tilde{c}_L squark and vice versa. We further note that if $M(\tilde{c}_L) = 1.5 \text{ TeV}$, Eqn. (13) $\lambda'_{223} \simeq 1.5$, which is close to the end of the perturbative regime. Our discussion, therefore, is restricted only to values of $M(\tilde{c}_L) \leq 1.5 \text{ TeV}$.

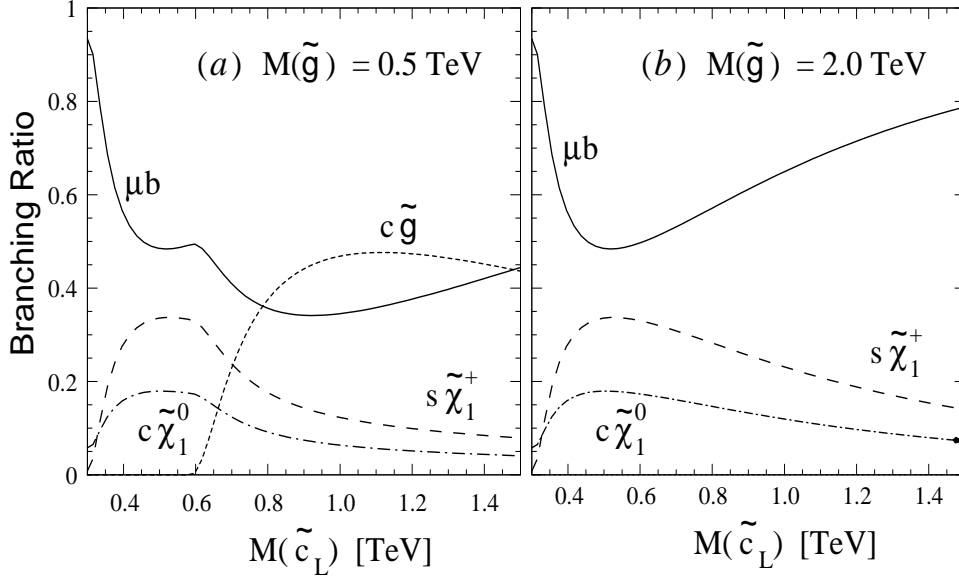


Figure 1: Illustrating the variation with the \tilde{c}_L mass of branching ratios for the processes $\tilde{c}_L \rightarrow \mu b$, $\tilde{c}_L \rightarrow c\tilde{g}$, $\tilde{c}_L \rightarrow s\tilde{\chi}_1^+$ and $\tilde{c}_L \rightarrow c\tilde{\chi}_1^0$ for the cases when (a) the gluino mass is 500 GeV and (b) the gluino mass is 2 TeV. For this illustrative plot, the other relevant MSSM parameters have been taken as $M_1 = 100 \text{ GeV}$, $M_2 = 300 \text{ GeV}$, $\mu = 1 \text{ TeV}$ while all squark (other than \tilde{c}_L) and slepton masses are set to 1.5 TeV.

A glance at Figure 1(a) will show that the direct RPV decay $\tilde{c}_L \rightarrow \mu b$ always dominates the chargino and neutralino channels, and is competitive with the gluino channel when that opens up. In the right panel, Figure 1(b) shows that $\tilde{c}_L \rightarrow \mu b$ remains the dominant channel everywhere if the gluino channel is kinematically disallowed. This is also the case where gluino production followed by cascade decays will enhance the μb signal. However, the LHC cross-sections will start falling for squark and gluino masses above a TeV.

If we now turn to the decay modes of the \tilde{c}_L through a gluino or a chargino or a neutralino, we note that new decay channels are opened here too because of R parity violation. Thus, a gluino or a neutralino can undergo a three-body decay through an off-shell \tilde{c}_L or \tilde{c}_L^* as

$$\begin{aligned} \tilde{g} \text{ or } \tilde{\chi}_i^0 &\rightarrow \bar{c} \tilde{c}_L \xrightarrow{\mathcal{R}} \bar{c} (\mu^+ b) \\ &\hookrightarrow c \tilde{c}_L^* \xrightarrow{\mathcal{R}} c (\mu^- \bar{b}) \end{aligned} \quad (14)$$

for all the neutralinos $i = 1, 2, 3, 4$ including the lightest one, which is usually the LSP. Similarly

the charginos can decay as

$$\tilde{\chi}_i^+ \rightarrow \bar{s} \tilde{c}_L \xrightarrow{\mathcal{R}} \bar{s} (\mu^+ b) \quad \tilde{\chi}_i^- \rightarrow s \tilde{c}_L^* \xrightarrow{\mathcal{R}} s (\mu^- \bar{b}) \quad (15)$$

where $i = 1, 2$. In such cases the final state will again contain a muon pair and a pair of b jets among other jets, but in this case we can no longer expect the $\mu - b$ invariant mass to peak at the \tilde{c}_L mass.

It is clear, therefore, that in a supersymmetric model with RPV, the possible decays of the \tilde{c}_L can occur through many channels, each of them producing a final state with a muon pair and two b quarks, with other quarks in the final state as well. At the parton level, a partial list is given below.

$$\tilde{c}_L \xrightarrow{\mathcal{R}} b \mu^+ \quad (16)$$

$$\begin{aligned} \hookrightarrow & s \tilde{\chi}_i^+ \xrightarrow{\mathcal{R}} s \bar{s} b \mu^+ \quad (i = 1, 2) \\ \hookrightarrow & s W^+ \tilde{\chi}_1^0 \rightarrow s \ell^+ \nu_\ell \tilde{\chi}_1^0 \xrightarrow{\mathcal{R}} s \ell^+ \nu_\ell (\bar{c} b \mu^+) \quad \text{or} \quad s \ell^+ \nu_\ell (c \bar{b} \mu^-) \\ \hookrightarrow & s q \bar{q}' \tilde{\chi}_1^0 \xrightarrow{\mathcal{R}} s q \bar{q}' (\bar{c} b \mu^+) \quad \text{or} \quad s q \bar{q}' (c \bar{b} \mu^-) \\ \hookrightarrow & s \ell^+ \tilde{\nu}_\ell \rightarrow s \ell^+ \nu_\ell \tilde{\chi}_1^0 \xrightarrow{\mathcal{R}} s \ell^+ \nu_\ell (\bar{c} b \mu^+) \quad \text{or} \quad s \ell^+ \nu_\ell (c \bar{b} \mu^-) \\ \hookrightarrow & s \nu_\ell \tilde{\ell}^+ \rightarrow s \nu_\ell \ell^+ \tilde{\chi}_1^0 \xrightarrow{\mathcal{R}} s \ell^+ \nu_\ell (\bar{c} b \mu^+) \quad \text{or} \quad s \ell^+ \nu_\ell (c \bar{b} \mu^-) \\ \hookrightarrow & c \tilde{\chi}_1^0 \xrightarrow{\mathcal{R}} c \bar{c} b \mu^+ \quad \text{or} \quad \bar{c} c \bar{b} \mu^- \\ \hookrightarrow & c \tilde{\chi}_j^0 \xrightarrow{\mathcal{R}} c \bar{c} b \mu^+ \quad \text{or} \quad \bar{c} c \bar{b} \mu^- \quad (j = 2, 3, 4) \\ \hookrightarrow & c Z^0 \tilde{\chi}_1^0 \rightarrow c \ell^+ \ell^- \tilde{\chi}_1^0 \xrightarrow{\mathcal{R}} c \ell^+ \ell^- (\bar{c} b \mu^+) \quad \text{or} \quad c \ell^+ \ell^- (c \bar{b} \mu^-) \\ \hookrightarrow & c q \bar{q} \tilde{\chi}_1^0 \xrightarrow{\mathcal{R}} c q \bar{q} (\bar{c} b \mu^+) \quad \text{or} \quad c q \bar{q} (c \bar{b} \mu^-) \\ \hookrightarrow & c h^0 \tilde{\chi}_1^0 \rightarrow c b \bar{b} \tilde{\chi}_1^0 \xrightarrow{\mathcal{R}} c b \bar{b} (\bar{c} b \mu^+) \quad \text{or} \quad c b \bar{b} (c \bar{b} \mu^-) \\ \hookrightarrow & c \ell^\pm \tilde{\ell}^\mp \rightarrow c \ell^+ \ell^- \tilde{\chi}_1^0 \xrightarrow{\mathcal{R}} c \ell^+ \ell^- (\bar{c} b \mu^+) \quad \text{or} \quad c \ell^+ \ell^- (c \bar{b} \mu^-) \\ \hookrightarrow & c \bar{\nu}_\ell \tilde{\nu}_\ell \rightarrow c \bar{\nu}_\ell \nu_\ell \tilde{\chi}_1^0 \xrightarrow{\mathcal{R}} c \bar{\nu}_\ell \nu_\ell (\bar{c} b \mu^+) \quad \text{or} \quad c \bar{\nu}_\ell \nu_\ell (c \bar{b} \mu^-) \end{aligned}$$

In the above, $\ell = e, \mu$, while $q\bar{q}$ refers to any pair of quarks $q = u, d, s, c, b$, and $q\bar{q}' = u\bar{d}$ or $c\bar{s}$. The use of alternatives marked ‘or’ corresponds to the Majorana nature of the neutralinos. Even if we assume that the gluino is heavier than the \tilde{c}_L , this list is illustrative, but not exhaustive, since there is considerable dependence on the mass spectrum of the sparticles, i.e. on the choice of supersymmetry-breaking parameters. For example, in the above decay chains, it has been assumed that all the squarks are heavier than the charginos and neutralinos, but if there is a light squark, additional decay channels of these particles will open up. Similarly, it has been assumed that the sleptons and sneutrinos are lighter than the $\tilde{\chi}_1^\pm$ and $\tilde{\chi}_2^0$ — but heavier, of course, than the LSP $\tilde{\chi}_1^0$. If this is violated, some of the above decay channels will be kinematically disallowed. Moreover, kinematics permitting, we can also have decay modes involving the heavier H^0 , A^0 and H^\pm states. Again, if the \tilde{c}_L can decay into a lighter gluino \tilde{g} many more channels are opened up. All these complications are, in fact, taken care of in our numerical studies, but it is not our purpose to display them here in an infinity of detail. Rather, the purpose of exhibiting the above list is to point out the following interesting facts, viz.

- The cascade decays occurring through RPC couplings will end up in a $\tilde{\chi}_1^0$ which will decay with equal probability into $c\bar{b}\mu^-$ and $\bar{c}b\mu^+$ final states, shown enclosed between parentheses in the last column of Eqn. (16). Given that the direct μb decay is always at the level of 40% or more (see Figure 1) it follows that the decay products of a \tilde{c}_L will contain a muon — of indeterminate sign — and a b quark or antiquark in at least 70% of the events, so long as there is a λ'_{223} interaction.
- When \tilde{c}_L 's are pair-produced and if they decay directly through the λ'_{223} coupling, the final state will contain a muon pair and two b jets. In this case, matching resonances will be seen in 2 of the 4 possible μb invariant masses. This is the only signal if the new physics consists of a leptoquark rather than squarks of RPV supersymmetry.
- If the \tilde{c}_L pair originates from the decays of a gluino pair, and then decays to a muon pair and two b jets, there is a possibility of same-sign muon pairs because of the Majorana nature of the gluino. Once again, there will be matching resonances in two μb invariant masses.
- If \tilde{c}_L 's are pair-produced, and decay mainly through RPC channels (e.g. through a gluino, chargino or neutralino), there will be no resonances in μb invariant masses, but one can have same-sign muon pairs arising from the neutralino LSP decays. An excess of muon pairs in the overall tally of same-sign lepton pairs is indicative of a λ'_{223} coupling, as against a RPC scenario, where lepton flavor universality is maintained.
- If the first step in the cascade decay of a \tilde{c}_L is through a chargino, decaying semileptonically, and the decay chain ends in a neutralino LSP decaying through RPV couplings, there exists a possibility of having same-sign leptons triads in the final state. These are so difficult to produce in other models that they practically constitute a ‘smoking gun’ signal for R parity violation [28].
- If a \tilde{c}_L pair arises in the decay of a gluino pair, and each \tilde{c}_L undergoes a decay beginning with a chargino and ending in a decaying neutralino LSP, one can even have spectacular events with lepton quartets of the same sign. Rare as such events will be, they will have no background(s) worth speaking of [28].

We now conduct a collider study for the λ'_{223} coupling by following the agenda set by the list of observations made above. The following section discusses the issue of resonances in μb invariant masses in the different cases explained above.

4 Scalar Resonances in Semileptonic Final States

In order to study \tilde{c}_L production and decay numerically we perform a Monte Carlo simulation of the relevant processes using the well-known event generator PYTHIA, which has an option to include RPV couplings at will, in addition to algorithms for fragmentation and jet formation as well as

initial- and final-state radiation of multiple soft gluons [29]. We also use the PYCELL algorithm inbuilt in the software to identify and segregate jets. While it is known that PYCELL is not the best of all the available jet identification algorithms, it is good enough for an exploratory study such as the present one. For the RPC part of the SUSY spectrum, we use the software SUSPECT [30]. Armed with these tools, we can now commence on a study of the RPV model in question and its signals.

Our analysis is carried out in two stages, as detailed below.

- We first consider the pair-production of \tilde{c}_L 's where each \tilde{c}_L decays to μb with unit branching ratio. This corresponds to the cases when (i) the SM is merely extended by the addition of a leptoquark⁵ decaying wholly to μb final states, and (b) the \tilde{c}_L is the LSP in an RPV version of the MSSM where all other SUSY particles are too heavy to have appreciable cross-sections. This is essentially the study presented in the current section, though we shall eventually consider some other scenarios.
- We then take up the case when the \tilde{c}_L is embedded in a RPV model with chargino(s), neutralino(s), and maybe gluinos, of comparable masses and cross-sections. This modifies the previous search in two ways, viz. (i) by reducing the branching ratio for $\tilde{c}_L \rightarrow \mu b$ from unity, and (ii) by introducing new \tilde{c}_L production modes through SUSY cascades. In this section we shall consider only the effects of the change in branching ratio. A detailed simulation of this scenario is carried out and described in the next section.

We first take up the case of a leptoquark, or a \tilde{c}_L LSP with other SUSY particles being very heavy (i.e. contributing neither to the signal or the background). We shall continue, however, to denote the particle as a \tilde{c}_L . Obviously, the cleanest signal for a leptoquark/squark \tilde{c}_L with a λ'_{223} coupling would arise when we observe two $\mu + b$ pairs, each with invariant mass peaking around the mass of the \tilde{c}_L . Since muons are easily identified at the LHC detectors, the viability of this signal is really controlled by the efficiency with which b jets can be tagged. A detailed study by the ATLAS Collaboration [31] shows that the efficiency of b tagging is in the neighbourhood of 40% for b jets with p_T less than about 300 GeV, but for higher p_T jets, the efficiency declines sharply. It follows that b tagging is a useful option only if the candidate jets have $p_T \lesssim 300$ GeV. When the p_T of the b -parton is significantly higher than this, we will have to treat b -jets on the same footing as light quark jets. We must, therefore, concern ourselves with the question: what are the final states of interest when a pair of \tilde{c}_L resonances decays into a muon pair and a pair of b -jets, which may or may not be tagged? A little reflection will show that there are four important possibilities, as detailed below.

1. The final state contains two muons and exactly two jets, both of which are tagged as b jets.

If we label the muons μ_1 and μ_2 by hardness (i.e. by the p_T value) and similarly label the b -jets as b_1 and b_2 by hardness, we can now construct four invariant masses, viz. $M(\mu_1 b_1)$,

⁵Actually two leptoquarks \tilde{c}_L and \tilde{b}_R , to fit the low-energy requirements.

$M(\mu_1 b_2)$, $M(\mu_2 b_1)$ and $M(\mu_2 b_2)$. Of these, one pair of invariant masses will correspond to the pair of \tilde{c}_L resonances, and hence will have similar values. We, therefore, construct the ratios

$$R_1 = \frac{M(\mu_1 b_1)}{M(\mu_2 b_2)} \quad \text{and} \quad R_2 = \frac{M(\mu_1 b_2)}{M(\mu_2 b_1)} \quad (17)$$

Of these, one ratio will be close to unity, since it will correspond to the correct choice of muon and b -jets, while the other will have some random value. We, therefore denote the correct ratio simply as R and impose a kinematic criterion requiring R to be close to unity. It is important to note that in tagging two b -jets with an efficiency around 40% each, we retain only 16% of the original events and hence, this signal may be rather small.

2. The final state contains two muons and 2 – 3 jets, of which two are tagged as b -jets.

This will correspond to the same process as above, but will include the cases where (i) one of the b -jets fragments into two, or (ii) there is an extra jet due to a gluon radiation from either the initial or the final state. Such cases would be excluded from the previous tag. Only the jets tagged as b -jets will be used to construct invariant masses and ratios thereof. This signal will thus resemble the previous one, but will be significantly enhanced.

3. The final state contains two muons and exactly two jets.

No b -tagging is employed in this case, and hence, the number of events will be much larger. As before, if we label the muons μ_1 and μ_2 by and the jets as J_1 and J_2 by hardness, we can now construct four invariant masses, viz. $M(\mu_1 J_1)$, $M(\mu_1 J_2)$, $M(\mu_2 J_1)$ and $M(\mu_2 J_2)$. Once again, we can construct ratios

$$R_1 = \frac{M(\mu_1 J_1)}{M(\mu_2 J_2)} \quad \text{and} \quad R_2 = \frac{M(\mu_1 J_2)}{M(\mu_2 J_1)} \quad (18)$$

and demand that one of them lie close to unity. This signal will be at least an order of magnitude higher than the similar case when we tag the b jets, for reasons explained above. However, it is no longer directly related to the coupling λ'_{223} but can be initiated by any of the λ_{22i} , where $i = 1, 2, 3$.

4. The final state contains two muons and 2 – 3 jets.

This is an inclusive case of the previous signal in which we allow an extra jet which may have been generated by QCD effects. Once again, no b -tagging is employed, and hence, if there are three jets, ordered J_1 , J_2 and J_3 by hardness, one has to construct six invariant masses $M(\mu_1 J_1)$, $M(\mu_1 J_2)$, $M(\mu_1 J_3)$, $M(\mu_2 J_1)$, $M(\mu_2 J_2)$, and $M(\mu_2 J_3)$, and six ratios

$$\begin{aligned} R_1 &= \frac{M(\mu_1 J_1)}{M(\mu_2 J_2)} & R_2 &= \frac{M(\mu_1 J_1)}{M(\mu_2 J_3)} & R_3 &= \frac{M(\mu_1 J_2)}{M(\mu_2 J_1)} \\ R_4 &= \frac{M(\mu_1 J_2)}{M(\mu_2 J_3)} & R_5 &= \frac{M(\mu_1 J_3)}{M(\mu_2 J_1)} & R_6 &= \frac{M(\mu_1 J_3)}{M(\mu_2 J_2)} \end{aligned}$$

of which one may be expected to peak near unity. Obviously this signal yields the most events, since there is no suppression due to b -tagging, and most of the QCD NLO effects are taken into account.

To avoid combinatorial backgrounds, this criterion may be also imposed in a cruder form, by assuming that J_3 , the softest of the jets will mostly arise from QCD effects rather than from a \tilde{c}_L decay. In this case, we can just construct R_1 and R_2 using the jets J_1 and J_2 and require one of them to be close to unity. In our numerical analysis, we have tried both approaches and found them to yield comparable efficiencies.

The four kinds of signal described above will be discernible only if the SM backgrounds are sufficiently small. The first and most obvious of these will arise from $t\bar{t}$ production, which has an NLO cross-section close to a nanobarn at the 14 TeV LHC. This is huge compared with the production cross-section for \tilde{c}_L squarks, which ranges from a few femtobarns to a few picobarns, depending on the squark mass. Moreover, the semileptonic decays of a top quark (or antiquark) will almost always contain a b -jet, and will have a 10.6% branching ratio to muons. Thus, there will be no dearth of final states containing a muon pair and a pair of b -jets in the decay products following a $t\bar{t}$ event, and it follows that it is a challenge to devise kinematic criteria which will restrict this background to manageable levels. Other backgrounds arise from the pair-production of W^+W^- , $W^\pm Z$ and ZZ accompanied by varying numbers of QCD jets. In particular, we could have, for example, $ZZ \rightarrow (\mu^+\mu^-)(b\bar{b})$ or $WZ \rightarrow \mu + \cancel{E}_T + \text{jets}$ or $W^+W^- + \text{jets} \rightarrow \mu^+\mu^- + \cancel{E}_T + \text{jets}$. Of course, our signal does not have substantial MET, but there will always be configurations with low MET among the background events, and even though these are rare, the cross-section for vector boson pair production (tens of picobarns) is enough to make their contribution significant. If a single Z , accompanied by a pair of b -jets, decays to $\mu^+\mu^-$, this can also be a sizable background.

It is clear, therefore, that the mere appearance of a muon pair accompanied by jets and little or no missing energy is not at all a clear signal for the particle in question. There are large irreducible SM backgrounds which must be taken into consideration. In principle, however, we have a panacea for all these backgrounds using our kinematic criterion imposed on the ratios R_1 and R_2 (see above). These will, in general, be close to unity only when a pair of \tilde{c}_L particles is produced and each of these then decay to a $\mu + b$ final state. For the $t\bar{t}$ and vector boson backgrounds, there is no *a priori* reason, except statistical fluctuations, for this ratio to lie in the neighbourhood of unity. This is illustrated in Figure 2, where we have plotted the signal and background distributions in the R which is closest to unity for the four classes of signal described above.

In order to generate Figure 2, we have made use of the following kinematic cuts and efficiency estimates.

1. The b -tagging efficiency is assumed to be $\epsilon_b = 0.4$ uniformly, for $p_T(b) \leq 300$ GeV. This is not a very bad approximation, since the variation in ϵ_b is rather small in the kinematic range in which the bulk of the b -jets are found in our analysis [31]. Similarly, we have assumed that the probability of mistagging a c -quark jet as a b jet is 10% and the probability of mistagging a light quark/gluon jet as a b -quark is 0.5%.
2. For the leptons (muons and electrons) we have imposed the following isolation cut: the

hadronic energy deposit in a cone of radius $\Delta R = 0.2$ around the lepton direction should be less than 10 GeV.

3. For the $2\mu + \text{jets}$ signal, we impose $\cancel{E}_T < 150$ GeV as well as

$$\frac{\cancel{E}_T}{M_{\text{eff}}} < 0.1 .$$

If we label the muons as μ_1, μ_2 and the jets as J_1, J_2 according to their transverse momenta p_T , then we also impose

$$p_T(\mu_1), p_T(J_1) > 100 \text{ GeV} , \quad p_T(\mu_2), p_T(J_2) > 50 \text{ GeV} ,$$

together with

$$M(\mu\mu), M(b\bar{b}) > 150 \text{ GeV} .$$

4. Finally we impose the kinematic criterion that if R be the ratio of invariant masses which lies closer to unity, then $0.5 < R < 1.8$.

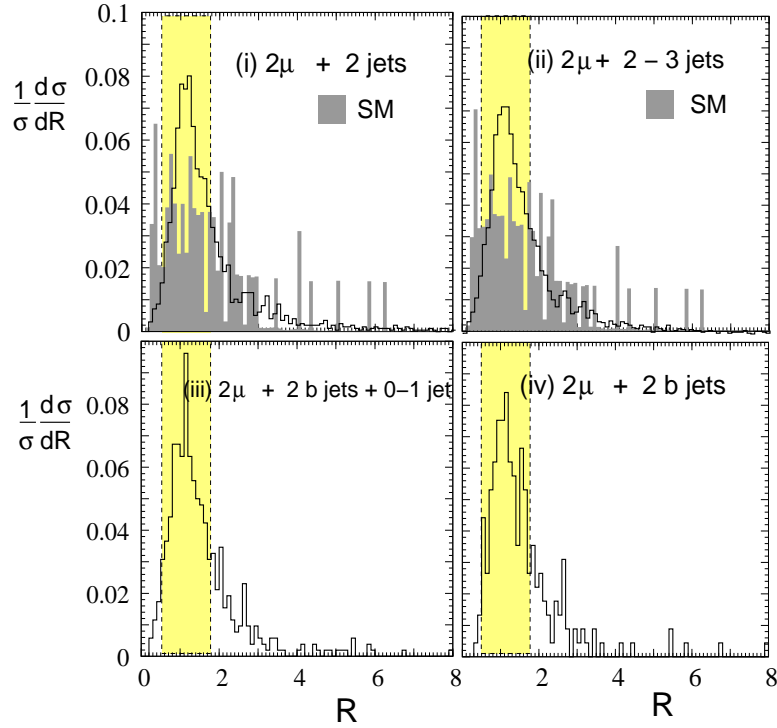


Figure 2: Normalized distribution in R , the ratio of invariant masses for the four cases where the final state contains two muons and (i) exactly two jets, (ii) up to three jets (iii) two b -jets and up to one extra jet, and (iv) exactly two b jets. The \tilde{c}_L mass is taken as 600 GeV. The shaded histogram in the upper panels represents the SM background. In the lower panels, the SM background is practically absent. The (yellow) shaded block between the broken lines indicates the cut on R .

The four panels in Figure 2 correspond to the four kinds of signal marked, i.e. running clockwise from the upper left panel: muon pair + 2 jets, muon pair + 2-3 jets, muon pair + 2 b jets and muon pair + 2 b jets + 0-1 jet. Normalized distributions have been shown in each case. The unfilled histograms indicate the signal and the dark grey shaded histogram represents the total SM

background. To generate these plots, the \tilde{c}_L mass has been taken as 600 GeV, but the distribution is not sensitive to reasonable variations in this parameter. No background is indicated in the lower two panels because these backgrounds lie below the level of a single event in a bin, assuming $\sqrt{s} = 14$ TeV and an integrated luminosity of 10 fb^{-1} . The broken lines indicate the range of R which we have considered as permissible for the signal, i.e. $0.5 < R < 1.8$.

A glance at Figure 2 will show that the signal is not as sharply peaked around unity as one would have expected from a resonant particle with a decay width of a few GeV at most. The reason is not far to seek: the reconstruction of the final state jets is fraught with uncertainties, arising from, for example, final state radiation, jet splitting/merging and/or undetected momentum in the form of soft jets or neutrinos. This results in a smearing-out of the peak, generating a long tail, which is apparent in all four panels of the Figure. However, most of the signal events are contained in the chosen range, viz. $R = 0.5 - 1.8$, as can be seen from the graph. It is somewhat unfortunate that this is also the area where a significant portion of the background lies, though that forms a much broader distribution. In fact, the cut $0.5 < R < 1.8$ removes about half of the SM background while leaving the leptoquark/RPV signal comparatively unscathed (even though a small tail towards large values of R does get affected).

One may question the rationale for imposing this criterion for the cases with b tagging, represented by the lower pair of boxes in Figure 2, given that the background is vanishingly small. The answer is that this criterion isolates events which are consistent with the hypothesis of a *pair* of heavy particles being produced and each then decaying into a muon and a b -jet. Events which satisfy this cut, therefore, may be considered candidates for a leptoquark/RPV signal. Thus the kinematic criterion on ratios, though it does not prove as powerful as one may have wished, certainly enriches the signal content in the selected sample of events.

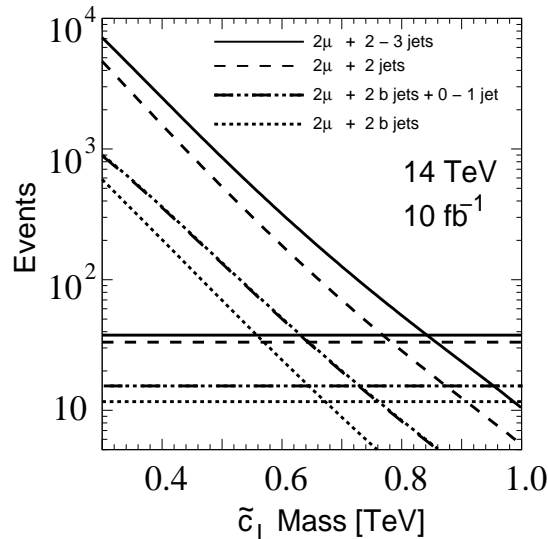


Figure 3: Illustrating the variation in total cross-sections as the mass of the leptoquark/squark \tilde{c}_L is varied, for the four kinds of signal considered in Figure 2, after implementation of the ratio criterion. The horizontal lines correspond to the SM background. We take $B(\tilde{c}_L \rightarrow \mu^+ b) = 1$ for the signal, as expected for a leptoquark.

In Figure 3 we show how the total cross-section for these four kinds of final state varies as the mass of the leptoquark/squark \tilde{c}_L increases from 300 GeV to 1 TeV, which is the LHC range of interest. These graphs make it clear that b -tagging is not a very good strategy, especially when the \tilde{c}_L mass increases above ~ 550 GeV. At the full energy of 14 TeV and an integrated luminosity of 10 fb^{-1} , the fact that tagging two b jets leads to a low efficiency factor of around 0.16 can be tolerated, since the statistics are large. However, in the early runs, the luminosity collection will be low and hence b -tagging will be a serious issue. In any case, a glance at Figure 3 shows that, as a search for new physics, the signals *without* b -tagging have a much better kinematic reach. For example, we can have a 5σ signal all the way up to $M(\tilde{c}_L) = 720(780)$ GeV for the signal with a muon pair and two jets (up to three jets). For even higher masses of the \tilde{c}_L , it is no longer worth considering the total cross-section, but we should look at the differential cross-section, where there will be resonant peaks in the muon-jet invariant mass construction.

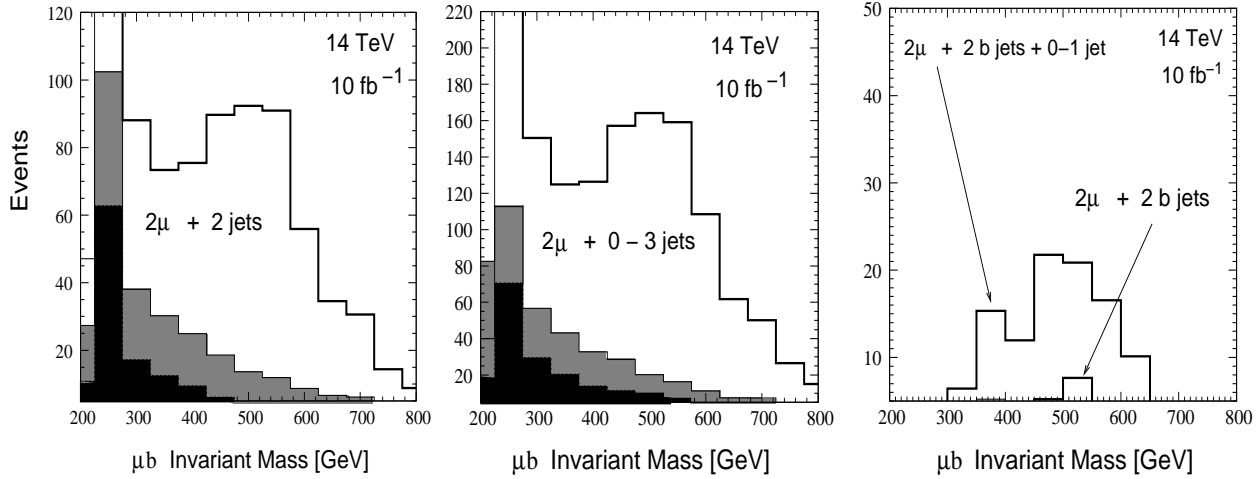


Figure 4: μb invariant mass distribution for the same leptoquark/squark signals as in Figure 2 with $B(\tilde{c}_L \rightarrow \mu^+ b) = 1$ as before. In each panel, the unshaded histogram indicates the signal added to the SM background, which is indicated by the dark-shaded histogram on the left and centre. The light-shaded histogram represents the 5σ fluctuation in the SM background. Note that the lower end of the plot corresponds to 5 events: in the panel on the right the SM backgrounds never rise above this minimum.

The resonant peaks described above are illustrated in Figure 4, where we have set $M(\tilde{c}_L) = 600$ GeV while $B(\tilde{c}_L \rightarrow \mu^+ b) = 1$ as expected in a leptoquark scenario. The panel on the left corresponds to the signal with a muon pair and exactly two jets: the distribution in the invariant mass of one of the μb pairs corresponding to $0.5 \leq R \leq 1.8$ has been shown (empty histogram). The SM background is the dark-shaded histogram and the 5σ fluctuation in the SM background is indicated by the light-shaded histogram. Clearly, a huge peak – though not at all a sharp one – does stand out from the background, indicating a squark mass very roughly around 500 GeV. This is about 100 GeV less than the choice $M(\tilde{c}_L) = 600$ GeV, and the discrepancy is clearly due to inaccuracies in jet identification and reconstruction. The situation is even better for the central panel, which shows the signal with a muon pair and up to three jets, with the same conventions as before. In this case, the peak again lies in the 500 – 550 GeV range, but is now significantly higher than the fluctuation in the SM background when compared with the plot on its left. On the other hand, the cases with b -tagging, which are virtually background-free and are shown in the panel on the right

in Figure 4, obviously fare best so far as significance is concerned. Unfortunately, the signal with a muon pair and exactly two b jets is barely discernible, even with 10 fb^{-1} of data. Note that we have set the lower edge of the graph at 5 events in 10 fb^{-1} of data. The signal where we allow an extra jet in addition to two b jets, however, does much better. Obviously, with the huge excesses shown in the first two panels of Figure 4, discovery of a leptoquark/squark with a 100% branching ratio to μb final states is pretty much assured. Even with 1 fb^{-1} of data, the significance of the signal can be estimated as around 5σ in the $2\mu+2$ jets channel, and 6.3σ in the $2\mu+(0-3)$ jets channel. Marginal improvements in the signal do arise if we relax the requirement that $0.5 < R < 1.8$, but eventually this does not change the significance by more than 10%.

We now come to the case when the \tilde{c}_L is a squark in a RPV model of SUSY with a more natural spectrum than that assumed above. As mentioned earlier, in this case, the signal is modified by (a) reduction of the branching ratio $B(\tilde{c}_L \rightarrow \mu b)$ due to the presence of competing channels (see Figure 1) and (b) the production of μ 's and b 's through cascade decays of other sparticles. Now, two cases arise. If the signal is considered purely as an *excess* of muons and b -jets, the background to this will come entirely from the SM, all SUSY contributions being considered part of the signal. On the other hand, if the presence of *resonances* in μb final states is considered as the signal (as described above), then the production of other SUSY particles through RPC modes will also constitute part of the background. Analysis of the first case is described in the next section. Here we concentrate on the second option.

Let us first consider the SUSY backgrounds to the resonant \tilde{c}_L signals, viz. (i) $2\mu + 2b$ jets, (ii) $2\mu + 2b\text{-jets} + 0\text{--}1$ jet, (iii) $2\mu + 2$ jets, and (iv) $2\mu + 0\text{--}3$ jets. In our RPV scenario, SUSY backgrounds will come from the variety of processes listed in Eqn. (16). These are listed for the \tilde{c}_L squark, but there will be similar processes for the other squarks as well (except for the first line, of course). A glance at the right-most column of Eqn. (16) will show that all these final states are hadronically rich, generally having at least four jets. If gluinos are heavier than squarks, they will decay to the same squark pairs with the addition of more jets in the final state. Thus, the signals for the resonant μb states will come only when there is substantial jet merging. Once subjected to the same kinematic cuts and the choice of a restricted band in the ratio R , as we have done for the signal and SM background, our numerical analysis shows that the sum total of all these backgrounds contributes only a minuscule amount to the SM background. Typically, in Figure 4 one would add not more than 1 – 2 events in each bin as shown. We have verified that this is true for the entire SUSY parameter space of interest. Thus, the direct effects of the remaining part of the SUSY spectrum are not of much significance in a search for \tilde{c}_L . Rather, the most important effect of having a lighter SUSY spectrum within the RPV paradigm will be to reduce the branching ratio $B(\tilde{c}_L \rightarrow \mu^+ b)$ from unity due to the opening up of new channels such as $\tilde{c}_L \rightarrow c + \tilde{\chi}_1^0$, $\tilde{c}_L \rightarrow s + \tilde{\chi}_1^+$ and $\tilde{c}_L \rightarrow c + \tilde{g}$, as illustrated in Figure 1. Since the four kinds of resonant signal require the presence of two \tilde{c}_L 's in the signal, the signal will be suppressed by $[B(\tilde{c}_L \rightarrow \mu^+ b)]^2$. A naive appraisal of total cross-sections (see Figure 3) using only this criterion will show that when $B(\tilde{c}_L \rightarrow \mu^+ b)$ falls below about 0.5, it will be difficult to isolate signals above

$M(\tilde{c}_L) \approx 600 - 700$ GeV.

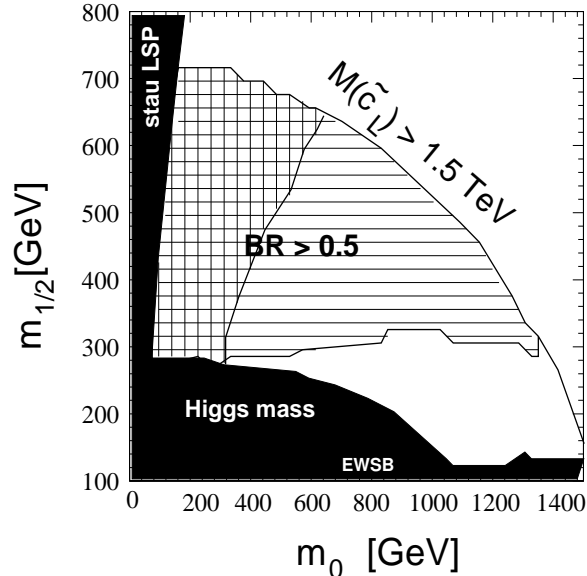


Figure 5: Illustrating the cMSSM parameter space and the region of interest [$M(\tilde{c}_L) < 1.5$ TeV] for squark resonances as discussed in this section. The other cMSSM parameters are fixed at $A_0 = 0$, $\tan \beta = 15$ and $\mu > 0$. The dark patches are ruled out by theoretical considerations or by direct searches as indicated on the Figure. The region hatched with horizontal lines has $B(\tilde{c}_L \rightarrow \mu^+ b) > 0.5$ and the region hatched with vertical lines has $M(\tilde{c}_L) < M(\tilde{g})$. Towards the lower right, we have a region with $B(\tilde{c}_L \rightarrow \mu^+ b) < 0.5$, where the gluino \tilde{g} is lighter than the squark \tilde{c}_L and hence the partial width for $\tilde{c}_L \rightarrow c + \tilde{g}$ dominates.

The situation is similar for studies of the μb and $\mu + \text{jet}$ invariant masses. Obviously the best channels to look for a \tilde{c}_L resonance in the given RPV model seem to be (i) the total cross-section for muon pairs with up to three jets, and (ii) the μb invariant mass for muon pairs with two b -tagged jets and possibly a third, untagged jet. In either case, with an integrated luminosity of 10 fb $^{-1}$ Figure 4 shows that a branching ratio of $\tilde{c}_L \rightarrow \mu^+ b$ as low as 0.5 can lead to an observable signal. The question, therefore, arises: how likely is this branching ratio to lie above 0.5? Obviously, the branching ratio will depend crucially on the SUSY mass spectrum and the couplings, including the mixing angle of gauginos and sfermions. Given the arbitrariness of the MSSM spectrum (which is exacerbated in the RPV case) one cannot give a definitive answer to this question. However, this issue is partially addressed by the plot shown in Figure 5 where we assume a minimal supergravity scenario with radiative electroweak symmetry breaking to get the well-known ‘constrained MSSM’ or cMSSM [32, 33]. In this scenario, we set the trilinear coupling $A_0 = 0$, $\tan \beta = 15$ and take the sign of the Higgsino mixing parameter μ to be positive. With this choice of soft SUSY-breaking parameters, the mass spectrum and running couplings are calculated at the electroweak scale, using the renormalisation group (RG) equations incorporated in the software SUSPECT. We then map the region in the m_0 – $m_{1/2}$ plane which leads to the desired branching ratio and exhibit our results in Figure 5. Apart from a small region at the bottom left of the panel, the rest of the parameter space is allowed by theoretical constraints and data from direct searches at the CERN LEP and Fermilab Tevatron. The region indicated with horizontal hatching corresponds, as marked, to a branching ratio $B(\tilde{c}_L \rightarrow \mu^+ b) > 0.5$, where the signal in Figure 4 will be discernible at the 5σ level. The overlapping region delineated with vertical hatching corresponds to the region where the gluino

\tilde{g} is heavier than the \tilde{c}_L , i.e. where gluino cascade decays will have a substantial \tilde{c}_L component. In the unshaded region on the lower right side of the graph, it is the \tilde{c}_L which is heavier than the gluino. Here, the dominant decay mode will be $\tilde{c}_L \rightarrow c + \tilde{g}$, as shown in Figure 1. The region outside the rough semicircle marked ‘ $M(\tilde{c}_L) > 1.5$ TeV’ is more-or-less kinematically disfavoured at the LHC, but its exclusion in the present graph is due to the fact that the coupling λ'_{223} becomes nonperturbative⁶ in this region.

It is not difficult to see why the hatched regions have the properties indicated above. In general, the gluino mass increases when $m_{1/2}$ increases and the squark mass increases when either $m_{1/2}$ or m_0 (or both) increases. It must be recalled that we assume that the RPV coupling λ'_{223} increases almost linearly as the mass of \tilde{c}_L increases. If the gluino is heavier than the squark, then the squark decays either into the direct RPV channel, which is a two-body decay to light states, or through RPC channels into charginos and/or neutralinos. If the latter prove to be heavier than the squark, they will undergo three-body decays which are suppressed; if they are lighter, the available two-body decays will have limited phase space when the squark-chargino/neutralino splitting is small. In such cases, which are more easily obtained at the left lower side of the Figure, the RPV channel dominates i.e. we have the large branching ratio indicated. However, as soon as the gluino becomes lighter than the squark, the situation changes, since the channel competing with $\tilde{c}_L \xrightarrow{\mathcal{R}} \mu + b$ is the strong interaction process $\tilde{c}_L \rightarrow c + \tilde{g}$, which becomes the dominant one. This behaviour is reproduced qualitatively as we change the other parameters, e.g. $\tan \beta$ running up to values as high as 40, A_0 of the order of a few hundred GeV to a TeV and $\mu < 0$. The plot shown here, therefore, is, in a sense, the most conservative one.

Finally we ask the question whether one could reproduce the signals for μb resonances in a model with RPC supersymmetry? Of course, there are better signals for SUSY in this case [23], but the question is of academic interest. We note that pp collisions can produce a pair of squarks or gluinos, each of which decay to charginos. If a muon appears among the decay products of each chargino, there will be enough jets in the cascade products of which some may easily be b -jets. For example, a typical decay chain could be $\tilde{q} \rightarrow q' + \tilde{\chi}_1^+ \rightarrow q' + (\mu^+ \nu_\mu \tilde{\chi}_1^0) \rightarrow \mu^+ + \text{jet(s)} + \cancel{E}_T$, which, repeated on either side with some cancellation of missing transverse momenta, could easily mimic the signal we are studying. This decay chain could also arise from a gluino: $\tilde{g} \rightarrow q + \tilde{q} \rightarrow qq' + \tilde{\chi}_1^+ \rightarrow \dots$. Generally RPC supersymmetry signals have a large MET component, but this is not true of all the events, and thus we have a residual background even after imposing a cut of $\cancel{E}_T < 150$ GeV. Keeping this in mind we have carried out a numerical simulation of an RPC model with a choice of several benchmark points in the parameter space accessible to LHC [23]. In each case, we find that after imposition of all the kinematic cuts and the selection criterion on the ratio R , very few events survive. In the left and middle panels of Figure 4 the deviation from the SM histograms is not enough to provide even a 2σ signal, while there are hardly any events at all in the right-most panel.

⁶See Eqn. (13) and the discussion following it.

To sum up, therefore, in the RPV model in question, there seems to be a strong case for predicting an observable squark resonance in the μb invariant mass when we look at final states with muon pairs accompanied by jets. If the parameters are right this can show up simply as an excess in the cross-section for a pair of resonances with equal mass. The signal is rather strong in a large part of the cMSSM parameter space, fading out somewhat as the squark and gluino masses grow heavier, but remaining at some noticeable, if not overwhelming, level almost to the kinematic reach of the machine. However, if a weak signal, say at the 2σ level, is seen, this may not be a convincing proof of the existence of SUSY with RPV. It would require corroboration from other signals. On such possible confirming signals we now focus our discussion.

5 The Non-resonant Case

In case the squark \tilde{c}_L is produced, but decays mostly through RPC channels — which is what happens when the \tilde{c}_L is heavier than the \tilde{g} and we have a small value of λ'_{223} — RPV will become apparent only at the last stage in the SUSY cascade decay, i.e. in the decay of the lightest supersymmetric particle (LSP) into a muon plus two jets. In Eq. (16), this will correspond to the decay modes indicated between parentheses in the extreme right column. As we have already noted, such final states arise at least 70% of the time and always contain a muon of indeterminate sign, together with multiple jets. When a gluon or a squark other than the \tilde{c}_L is produced, the decay channels will be very similar, except for the direct decay into a μb pair. These will decay through RPC cascades into the LSP $\tilde{\chi}_1^0$, which will then decay into a muon, a b jet as well as other jets and MET. When a pair of gluinos or squarks is produced, these will be produced with double the multiplicity for every particle, including jets. Hence, even if we do not have an observable μb resonance, an excess of μ 's and b -jets in the final state will be a clear indicator of the RPV model in question.

It may be noted that the signals discussed in this section are not so crucially dependent on the actual value of the λ'_{223} coupling, since the LSP has essentially only one decay mode. This discussion will, therefore, be largely valid *even if we do not impose a scaling of λ'_{223} with $M(\tilde{c}_L)$* as was done in the previous section. This is an example of an analysis which holds irrespective of whether we correlate low-energy effects with the high-energy frontier, and is, in a sense, more robust than the signals discussed in the previous section.

To showcase the above, we choose a particular signal out of the many possible ones. We trigger on a final state with a muon pair (irrespective of sign), only one tagged b -jet and a complement of *at least* 3 more jets, making a total of 4 jets. This final state will receive contributions from almost all the cascade decays ending in an LSP listed in Eq. (16). The resonant signal, when it dominates, will also contribute to this final state, when it arises from the decay of a pair of gluinos, but not, in general, if a $\tilde{c}_L\tilde{c}_L^*$ pair is produced directly. Some small contributions may still arise in the last case if extra jets are generated by radiative or jet-splitting effects, but these will not change the

qualitative features of this signal, and in any case, are taken care of in our analysis which uses the event generator PYTHIA.

The above signal is not, however, free from backgrounds. The principal background will arise from $t\bar{t}$ production, with its huge NLO cross-section: almost up to a nanobarn. If both the top quarks decay semileptonically, to a muon, a b -jet and missing energy, we shall have a final state short by two jets from the given signal. Such extra jets can easily be generated by radiative or jet-splitting effects, as mentioned above, and though it will lead to an automatic suppression by at least $\mathcal{O}(\alpha_s^2)$, as a fraction of the enormous $t\bar{t}$ cross-section it will still be a formidable background to the signal under consideration. Other obvious contributors will be a final state with a Z boson and four jets, where at least one of the jets is a b jet and the Z decays to a $\mu^+\mu^-$ pair, or a W^+W^- plus four jets, where both W 's decay to muons and at least one of the jets is a b jet. These are much smaller, however, than the $t\bar{t}$ contribution, and will not affect the signal overmuch. It is true that in all these effects, the muon- p_T will be somewhat restricted by the fact that it arises from the decay of an on-shell W/Z boson, but this is not of much help, since the muons in the signal, except for the very few which arise from the decay of a resonant \tilde{c}_L , are a product of the decay of the LSP, which may not be significantly heavier than the W boson. Moreover, the p_T distribution will be much smeared-out by the kinematics of the rather complicated final state, and may not look very different, whether the source is a $t\bar{t}$ pair, or a SUSY cascade decay.

The viability of this signal is illustrated in Figure 6. In our numerical analysis, the following kinematic cuts were imposed.

1. The muons were required to have transverse momentum $p_T(\mu) > 20$ GeV.
2. The jets were ordered as J_1, J_2, \dots according to their p_T values, after which we imposed

$$p_T(J_1) > 100 \text{ GeV} \quad p_T(J_i) > 50 \text{ GeV for } i = 2, 3, 4, \dots$$

3. The transverse sphericity σ of each event was required to satisfy $\sigma > 0.2$.

No restrictions were made on the missing energy and momentum of the events; likewise, the pairwise invariant masses were allowed to vary freely. Finally, we plot the μb invariant mass, taking the harder of the two muons in the signal⁷.

In Figure 6, as in Figure 4, the dark-shaded histogram represents the SM background, principally originating from $t\bar{t}$ production, and the light-shaded histogram represents its possible 5σ fluctuations. The unshaded histogram drawn with a solid line represents the prediction of the RPV model, where the entire SUSY spectrum is generated in a cMSSM with $m_0 = 100$ GeV, $m_{1/2} = 300$ GeV, $A_0 = 0$, $\tan\beta = 15$ and $\text{sgn}(\mu) = +1$. In this scenario, we predict $M(\tilde{c}_L) \simeq 650$ GeV and $M(\tilde{g}) \simeq 740$ GeV. To keep the low-energy solutions consistent, we scale $\lambda'_{223} = 0.65$, which is comparable to the electroweak $\text{SU}(2)_L$ coupling g . This set of parameters determines everything

⁷We have checked that taking the softer muon does not change the qualitative features of the graph.

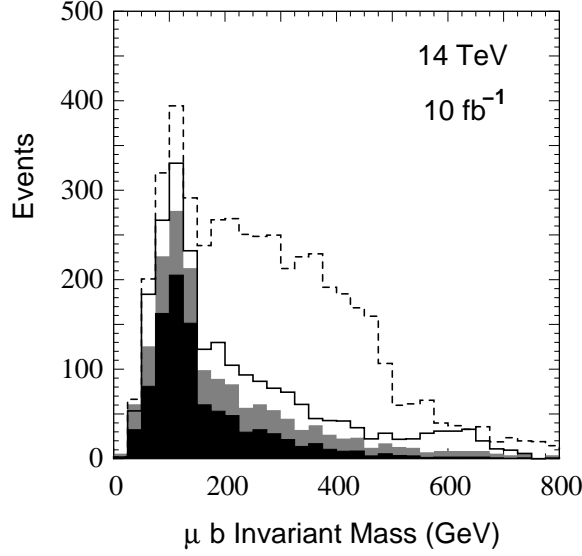


Figure 6: μb invariant mass distribution for the signal with a muon pair and ≥ 4 jets of which at least one is a b -jet. The solid dark-shaded histogram represents the SM background, while the solid light-shaded histogram represents its possible fluctuations at the 5σ level. The unshaded histogram with a solid line represents the RPV signal when the gluino is heavier than the \tilde{c}_L , while the unshaded histogram with the broken line represents the RPV signal when the \tilde{c}_L is heavier than the gluino. Values of the SUSY parameters in both cases are given in the text.

in the model, from production cross-sections to branching ratios, and the above plot shows that we predict a clear signal above the 5σ discovery level at the LHC. The signal shows a peaking behaviour around 100 GeV, which may be attributed to the cases where the muon and b -jet arise from the decay of the neutralino $\tilde{\chi}_1^0$ LSP, which has a mass in just that ballpark. There is also a modest peaking around 600 GeV, which may be attributed to the \tilde{c}_L resonance, and is the analogue, for this more-inclusive signal, of the sharper peaks shown in Figure 4. The number of events in this region, with the luminosity projection of 10 fb^{-1} is much larger than the background, and hence, if seen, would be a ‘smoking gun’ signal for new physics beyond the SM.

If we consider a situation where the gluino is lighter than the squark \tilde{c}_L we should expect no such peak around $M(\tilde{c}_L)$, and indeed, this is the case with the unshaded histogram drawn with broken lines in Figure 6. In this case, all the parameters have been kept at the same values as before, with the exception of the gluino mass, which has been reduced (by hand, as it were) from 740 GeV to 620 GeV⁸. At 620 GeV, the gluino is lighter than the \tilde{c}_L at 650 GeV, and hence the \tilde{c}_L will decay principally into $c + \tilde{g}$. The cascade decays will now resemble the RPC scenario, with an enhanced gluino production due to the smaller mass, and all these decays will end in $\tilde{\chi}_1^0$ LSPs, which will then decay through λ'_{223} . The muon and b -jet will thus arise from these end-products of SUSY cascades, which explains why we get copious numbers of signal events as shown by the histogram in Figure 6. Of course, the huge increase in the signal may be attributed in increased pair-production of the lighter gluino in this case, and may not be as large over the full cMSSM parameter space, but the point which we would prefer to stress is that we get a substantial signal in *both* scenarios,

⁸Obviously, this is not consistent with the cMSSM spectrum, but it can be generated easily enough in a non-universal scenario where the $\text{SU}(3)_c$ gaugino mass is taken different from those in the electroweak sector.

whether there is a \tilde{c}_L resonance or not. This signal will fade out as the squarks and gluinos grow heavier, as is true with all SUSY signals at the LHC, but in this case, it is not sensible to go to very high values of the \tilde{c}_L mass, since then one cannot get large FCNC effects without pushing λ'_{223} towards the non-perturbative regime. For $M(\tilde{c}_L) \gtrsim 1$ TeV, therefore, it is doubtful if RPV can simultaneously be observed in low-energy processes and at the LHC.

It is interesting to ask how we can tell if the non-resonant signal considered in this section arises from SUSY of the RPC or RPV type. Actually this distinction is very easy to make, for the RPC model will produce roughly equal numbers of e^\pm and μ^\pm in the final state, since these will mainly arise as decay products of W, Z bosons or near-degenerate sleptons. On the other hand, RPV decays of the $\tilde{\chi}_1^0$ LSP through a λ'_{223} coupling will inevitably produce a huge excess of muon final states as compared with electron final states. This is illustrated in Table 1 below, where the number of events is exhibited with both RPC and RPV cases, for ee , $e\mu$ and $\mu\mu$ (of arbitrary sign) final states accompanied by jets and MET, as considered above. We have also imposed the additional cut $\cancel{E}_T < 150$ GeV, which helps to suppress the RPC signal compared with the RPV one.

	N_{ee}	$N_{e\mu}/N_{ee}$	$N_{\mu\mu}/N_{ee}$
RPC	30	1.1	1.15
RPV	53	7.5	41.0

Table 1: Comparing similar final states with electrons and muons in the case of RPC and RPV varieties of SUSY. The numbers N correspond only to the signal. Parameter choices are the same as used to generate the solid line histogram in Figure 6. We take $\sqrt{s} = 14$ TeV and $\mathcal{L} = 10 \text{ fb}^{-1}$ for our simulation.

It is obvious from Table 1 that irrespective of the actual numbers, the flavour ratios obey the hierarchy

$$\left(\frac{N_{e\mu}}{N_{ee}}\right)_{\text{RPV}} > \left(\frac{N_{e\mu}}{N_{ee}}\right)_{\text{RPC}} \quad \left(\frac{N_{\mu\mu}}{N_{ee}}\right)_{\text{RPV}} \gg \left(\frac{N_{\mu\mu}}{N_{ee}}\right)_{\text{RPC}} \quad (19)$$

i.e. there is a huge relative excess in muonic final states compared to electronic final states in the RPV case. While the ratios exhibited in Table 1 will vary considerably when we move to other points in the parameter space, the *qualitative* feature in Eqn. (19) will generically be reproduced, and may be taken as a ‘smoking gun’ signal for R-parity violation through a λ'_{223} coupling.

6 Same-Sign Leptons and their Significance

In the two previous sections we have discussed searches for RPV in certain final states and invariant mass distributions, using mainly the kinematic properties of the SUSY particle spectrum. We now turn to an important *dynamic* property, viz. the fact that the charge-neutral gauginos – gluinos and neutralinos – are fermions of Majorana type, i.e. they are their own antiparticles. No such particles are known to exist in the SM; in fact, a multiplicity of Majorana particles is a special feature of SUSY models. In the context of our analysis, therefore, we should expect some unique features

arising from the Majorana property and it turns out that we can expect some really spectacular signals which are the subject of discussion in the current section.

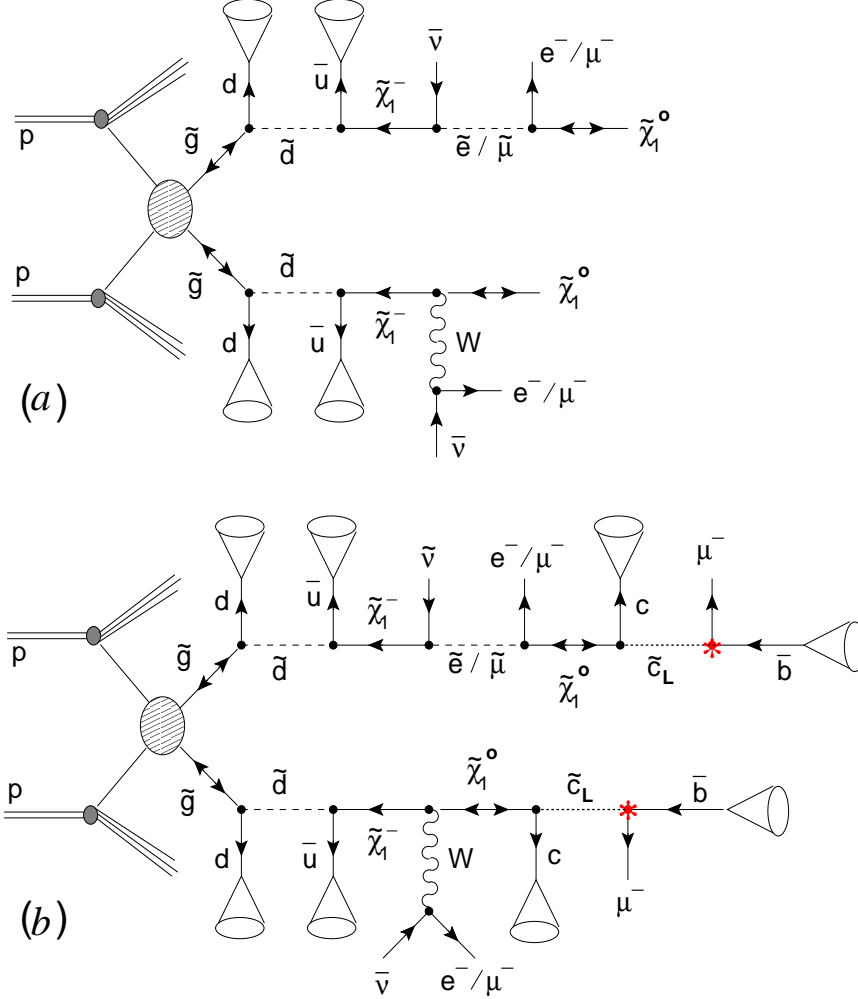


Figure 7: Same-sign lepton production at the LHC in (a) RPC and (b) RPV models. In (a) the final state is a same-sign lepton pair (SSLP), together with jets and MET; in (b) the final state is a same-sign lepton quartet (SSLQ), together with jets and MET. The RPV couplings correspond to the vertices marked with asterisks on the extreme right in (b). Little cones indicate jets and the dotted (not dashed) lines indicate virtual (off-shell) states. In (b), if the W boson decays hadronically, the final state will be a same-sign lepton triad (SSLT), together with jets and MET.

Before discussing the specific effects in the current RPV model, let us briefly review the predictions of the RPC version of SUSY with regard to Majorana fermions. This is illustrated in Figure 7(a) as arising from the gluino decay chain

$$\tilde{g} \longrightarrow q + \tilde{q} \longrightarrow q + q' + \tilde{\chi}_1^\pm \longrightarrow q + q' + \ell^\pm + \cancel{E}_T$$

where the decay of the chargino can take place through two different channels as shown. In the Figure, the little cones indicate hadronic jets and the clashing arrows indicate Majorana fermions. The Majorana nature of the neutralino LSP $\tilde{\chi}_1^0$, however, has no effect, since it contributes only to MET. However, the gluinos \tilde{g} can give rise to identical charginos on either side, leading to same-sign lepton pairs (SSLP). Here, as before, we consider only the charged leptons e^\pm and μ^\pm . Of course, there can also be opposite-sign leptons in these decay chains, but these will have large SM

backgrounds, whereas there is hardly any SM background to the same sign dilepton signal. Note that unless there is a large mass-splitting between the selectron and the smuon, the probability for a chargino to decay to an electron is roughly the same as its probability to decay to a muon, and hence same-sign ee , $\mu\mu$ and $e\mu$ pairs would arise in the rough proportions 1:1:2 in the RPC version of SUSY. If we consider only gluino production, then $\ell^+\ell^+$ and $\ell^-\ell^-$ pairs will be produced in equal proportions, but when squark pair production or squark-gluino pairs are considered at a pp collider, $\ell^+\ell^+$ pairs dominate over $\ell^-\ell^-$ pairs [22]. The flavour ratio is, however, maintained, irrespective of sign, and this is what our analysis will focus upon.

The situation becomes much more interesting if R parity is violated [28]. For, as we have seen in this case, the neutralino LSP $\tilde{\chi}_1^0$ can decay through a virtual \tilde{c}_L into a final state with a μ^\pm and two jets. Both signs of the muon are permitted, because of the Majorana nature of the $\tilde{\chi}_1^0$, which here assumes an important role, unlike the previous case. The decay chain shown in Figure 7(a) is now extended, as shown in Figure 7(b), by the decay of the LSP's, and it can be seen, that, in addition to the $e^\pm e^\pm$, $\mu^\pm \mu^\pm$ and $e^\pm \mu^\pm$ pairs arising from the chargino decay, we can add on a same-sign $\mu^\pm \mu^\pm$ pair from the neutralino decay — the result being same-sign lepton *quartets* (SSLQ) such as $e^-e^-\mu^-\mu^-$ or $e^-\mu^-\mu^-\mu^-$ or even $\mu^-\mu^-\mu^-\mu^-$ (and, of course, their positively-charged counterparts). It is also possible for one or more of the charginos to decay hadronically, i.e.

$$\tilde{\chi}_1^\pm \rightarrow \tilde{\chi}_1^0 + W^\pm \rightarrow \tilde{\chi}_1^0 + q\bar{q}$$

Insertion of this in place of *one* of the chargino decays shown in Figure 7(b) would lead to a prediction of same-sign lepton *triads*, (SSLT) of the form $e^-e^-\mu^-$, $e^-\mu^-\mu^-$ or $\mu^-\mu^-\mu^-$ (and their positively-charged counterparts). In fact, since the hadronic branching ratio of the chargino is generally larger than its branching ratio to leptons e, μ , one may expect many more events with SSLT than SSLQ. The most probable channel will be for both the charginos to decay hadronically, in which case, it is still possible to have SSLP — $\mu^\pm \mu^\pm$ — from the decays of the neutralinos. Thus, in an RPV model one would predict [28] the simultaneous existence of SSLP, SSLT and SSLQ, in decreasing order of cross-section. All have vanishingly small backgrounds in the SM — typically below 10^{-1} fb for SSLT and even lower for SSLQ, as shown in Ref. [28]. In the RPC versions of SUSY, all of SSLP, SSLT and SSLQ will arise, but, as discussed above, the number of muonic events will be roughly equal to the number of electronic events for the RPC case, unlike the RPV case considered here, where muons will be overwhelmingly dominant. We shall take up this point in more detail in the following discussion.

We have made a numerical study of the SSLP, SSLT and SSLQ signals at the LHC, using, as before, the event generator PYTHIA. For these studies at $\sqrt{s} = 14$ TeV, the following kinematic cuts were imposed:

1. For the SSLP case, we imposed

$$p_T(\ell) > 20 \text{ GeV}$$

for both the leptons. Up to 4 accompanying jets were considered, and the jets were ordered

as J_1, J_2, \dots according to their p_T values, after which we imposed

$$p_T^{J_1} > 100 \text{ GeV} \quad p_T^{J_i} > 50 \text{ GeV for } i = 2, 3, 4.$$

The transverse sphericity σ of each event was also required to satisfy $\sigma > 0.2$. No cut was imposed on the MET.

2. For the SSLT case, we imposed a cut

$$p_T(\ell) > 20 \text{ GeV}$$

for all three leptons, and no other cuts on jets and/or MET.

3. For the SSLQ case, the cut on the lepton transverse momentum was reduced to

$$p_T^\ell > 10 \text{ GeV} .$$

For studies at 7 TeV, we imposed $p_T^\ell > 10 \text{ GeV}$ for both SSLT and SSLQ signals.

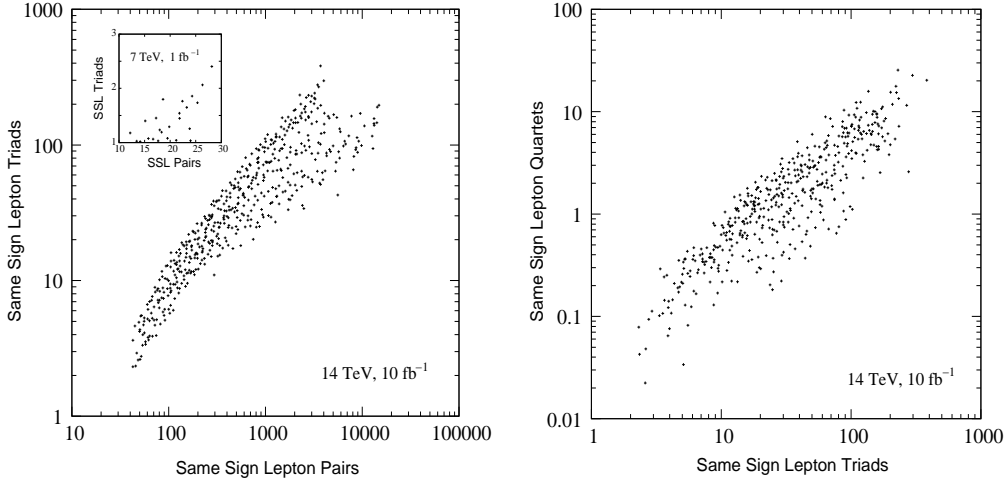


Figure 8: Same sign lepton production at the LHC for 10 fb^{-1} luminosity at the 14 TeV run. The left panel shows the number of same-sign triads (SSL) versus same sign pairs (SSLP), while the right panel shows the number of same-sign quartets (SSLQ) versus triads (SSLT). Each point represents a set of vales of the cMSSM parameter space. The inset box shows the SSLT-SSLP plot for 1 fb^{-1} luminosity at the 7 TeV run.

Our results are presented in Figure 8. In the left panel, we plot, for $\sqrt{s} = 14 \text{ TeV}$ and an integrated luminosity of 10 fb^{-1} , the number of events with SSLT versus the number of events with SSLP, while the parameters of the model are sampled randomly over the ranges:

$$m_0 = 0.1 - 2.0 \text{ TeV} \quad m_{1/2} = 0.1 - 1.5 \text{ TeV} \quad A_0 = 0, \tan \beta = 15, \mu > 0 .$$

The mass spectrum for this model is generated as before, assuming the cMSSM. Given this model, each point on this plane represents a particular choice of m_0 , $m_{1/2}$ and $\tan \beta$, while we set $A_0 = 0$ and take $\mu > 0$. The corresponding mass spectrum is required to satisfy LEP constraints on the light Higgs boson mass as well as the requirement that $M(\tilde{\chi}_L) < 1.5 \text{ TeV}$, which defines our region of interest. It may be seen that the predicted points lie in the neighbourhood of a straight line with

slope of approximately 0.1 — this is just the ratio between the leptonic and hadronic branching ratios of the chargino, as the above discussion would lead us to expect. What is more important, however, is that fact that Figure 8 tells us that for every 10 SSLP events seen, we should expect at least one SSLT event. The numbers could be as high, for some regions of the parameter space, as a few thousand SSLP events and around a hundred SSLT events.

The situation for $\sqrt{s} = 7$ TeV and a data sample of 1 fb^{-1} is shown in the box inset on the left side of Figure 8. The sparseness of points is an artifact of the fact that the whole parameter space was scanned with the same resolution as in the 14 TeV case, out of which just a small sliver contributes to the 7 TeV signal. What is exciting, however, is that it is possible, if the parameters happen to be just right, that we could see some 10–25 SSLP events accompanied by just one or two SSLT events. Should such a signal be seen, we would have found solid evidence for SUSY, and just a tantalizing hint for RPV. This is as far as the 7 TeV run can go; clinching evidence will have to wait for the 14 TeV run.

If the SSLT events are roughly an order of magnitude rarer than the SSLP events, then we should expect the SSLQ events to be another order of magnitude rarer still. This is, in fact, the case, as is shown in the right panel in Figure 8. SSLQ events are not predicted at the 7 TeV run, so this panel is exclusively for the $\sqrt{s} = 14$ TeV and 10 fb^{-1} run. Obviously, if we see less than 10 SSLT events, we should not expect to see any SSLQ events, but, as we have seen before, if the parameter space turns out to be favourable, we may see as many as a hundred SSLT events with up to 10 SSLQ events. Such spectacular signals would immediately indicate the presence of RPV, as envisaged in this model.

We now come to the issue of distinction of SSLP and perhaps SSLT signals arising in this model versus those arising in conventional RPC SUSY. Studies of the latter has been carried out in Ref. [22] and, more recently, in Ref. [34], and it is not our purpose, in this work, to repeat such analyses. Rather, we take up the question: if we do indeed observe SSLP and SSLT events⁹ how can we tell if the underlying SUSY model is of the RPC or RPV type? The answer is actually very simple: as we have seen, in RPC versions of SUSY, cascade decays tend to end in equal numbers of electrons and muons, whereas in our RPV model with a large λ'_{223} coupling, muons have a tendency to dominate. This has already shown up in a different context in Table 1, but in the case of same-sign leptons it can be used in an equally dramatic way.

Taking up the case of SSLP first, we have already noted that same-sign ee , $\mu\mu$ and $e\mu$ pairs would arise in the rough proportions 1:1:2. This encourages us to construct the ‘muon ratio’

$$Q^{(2)} = \frac{4\sigma_{\mu\mu}^{\text{SS}}}{\sigma_{ee}^{\text{SS}} + \sigma_{e\mu}^{\text{SS}} + \sigma_{\mu\mu}^{\text{SS}}} \quad (20)$$

and predict $Q^{(2)} \approx 1$ in the RPC model. Similarly, for the SSLT case, we can construct a ‘muon

⁹SSLQ events are a rare option that almost never arises in RPC SUSY for an integrated luminosity of 10 fb^{-1} .

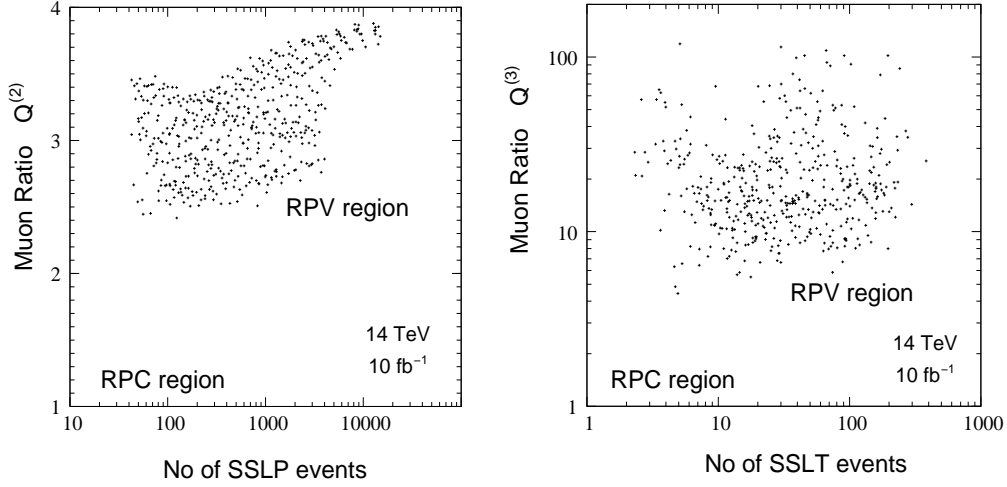


Figure 9: ‘Muon Ratios’ constructed for the SSLP and SSLT samples for the RPV model. The parameter ranges are identical with those of Figure 8. The left panel is for SSLP signals, whereas the right panel is for SSLT signals. Note the clear separation between the RPV and RPC regions indicated on both panels.

ratio’

$$Q^{(3)} = \frac{\sigma_{\mu\mu\mu}^{SS} + \sigma_{e\mu\mu}^{SS}}{\sigma_{eee}^{SS} + \sigma_{ee\mu}^{SS}} \quad (21)$$

with an RPC prediction $Q^{(3)} \approx 1$. It only remains, then, to see what these ratios work out to in the RPV model, and this is exhibited in Figure 9. It may be noted that within the given parameter choice, there will always be at least 40 SSLP events, which allows a meaningful construction of the $Q^{(2)}$ variable, which is seen never to drop below 2.4. The situation is not so clear for SSLT events, where the prediction drops to as low as 2 events, where, obviously, construction of the $Q^{(3)}$ variable is not meaningful (unless the luminosity goes up by about an order of magnitude). However, for the part of the parameter space where we get 10 or more events, the ‘muon ratio’ $Q^{(3)}$ never drops below 5, which is a far cry from the RPC prediction – close to unity. Thus, distinction between RPC SUSY and the model discussed in this work is a simple matter for SSLP signals and for SSLT signals if the parameters are favourable.

The above discussion would be incomplete without a discussion of which part of the parameter space in this model would be excluded if SSL signals are not seen at the LHC. This is shown in Figure 10. The left panel corresponds to the $\sqrt{s} = 14$ TeV and 10 fb^{-1} run, while the right panel is for the $\sqrt{s} = 7$ TeV and 1 fb^{-1} run. As before, we work in the cMSSM framework and show the m_0 – $m_{1/2}$ plane with $\tan\beta = 15$, $A_0 = 0$ and $\mu > 0$. The dark shaded regions are ruled out by theoretical considerations or by direct searches, as marked on the Figure. The same conventions are followed for both panels. The regions where one can expect at least *one* SSLP event are indicated by vertical hatching, the regions corresponding to at least *one* SSLT event are indicated by horizontal hatching and the region (there is no such region in the 7 TeV case) corresponding to at least *one* SSLQ event are indicated by slanting hatching.

Even a glance at Figure 10 will show that SSLP events are predicted over most of the kinematically

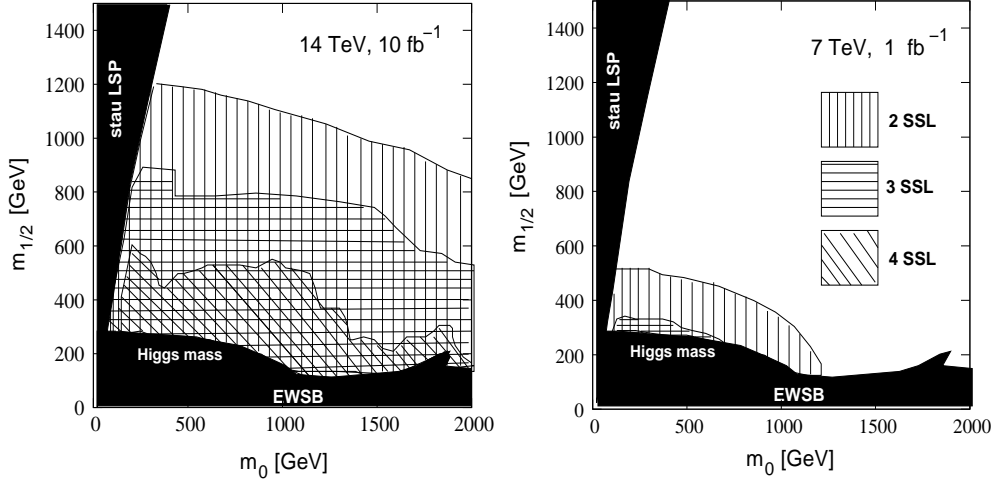


Figure 10: Same-sign lepton production at the LHC. The left panel corresponds to 10 fb^{-1} luminosity at the 14 TeV run and the right panel corresponds to 1 fb^{-1} luminosity at the 7 TeV run. Dark regions are ruled out by theoretical considerations or by direct searches. Regions hatched with vertical, horizontal and slanting lines correspond to viable signals with lepton pairs, triads and quartets respectively.

accessible parameter space of the cMSSM-based RPV scenario at the LHC. The region thus mapped (vertical hatching) is somewhat more extensive than in the RPC case, because that requires the charginos to decay to leptons rather than jets. However, the best exclusion plots in the RPC case are obtained not from SSL signals but from a 4-jets plus MET signal [23]. In our RPV model the origin of SSLP is from the neutralino decay which has no competing channel (except the RPV one to $\nu_\mu s \bar{b}$). However, mere discovery of SSLP events with a somewhat larger cross-section could perhaps be explained by some variant of the cMSSM. What is more interesting is that SSLT events are also predicted over a wide swath of the parameter space, and these could prove the clinching evidence for RPV as a phenomenon. If the parameters are very favourable, i.e. we have a SUSY-around-the-corner scenario, we may eventually be able to see SSLQ events as well. Such events would surely satisfy even the most die-hard sceptic of the existence of RPV. However, as the corresponding patch in the parameter space is small, one should not bank upon it. Similarly, SSL signals will appear only for a very small patch of the parameter space in the panel on the right, i.e. for the 7 TeV run, and this indicates that an RPV discovery there would require the parameters to be in just the right ballpark.

7 Summary and Conclusions

In this work, we build on the premise that new physics beyond the Standard Model, may affect low-energy processes and at the same time lead to direct searches at the LHC. While it is true that there exists no measurement at low energies which is in direct contradiction with the Standard Model prediction within a reasonable level of experimental error, it is also true that we are on the threshold of making low-energy measurements, which may well be much larger than the Standard

Model estimates, and would, therefore, be better understood if we assume the existence of new physics. We focus on a set of such phenomena, viz., neutrino masses, rare branching ratios of the tau lepton, the phase in B_s - \bar{B}_s mixing, and the decay $D_s \rightarrow \ell \nu$, which could collectively indicate the existence of a leptoquark with equal λ'_{223} and λ'_{323} couplings, or alternatively, a supersymmetric model where R-parity is violated by just this pair of couplings, without falling foul of the muon anomalous magnetic moment. Current experimental data are compatible with a coupling strength $\lambda'/\tilde{m} \approx 1 \text{ TeV}^{-1}$, where \tilde{m} is the mass of the leptoquark or the R-parity-violating squark. As this is just the scale at which the LHC processes are due to take place, we then set out to explore the consequences of having such a model in the context of LHC signals.

We have explored three kinds of LHC signals. The first would be important if the new physics consists of a leptoquark, with only the couplings mentioned above. These would be produced copiously at the LHC because of their strong interactions, and their characteristic decays to a lepton and a jet could then be exploited to construct pairs of resonances, whose observation at the LHC would be a simple matter, as we demonstrate by a detailed Monte Carlo simulation of the signal vis-à-vis its principal backgrounds. If, however, the new physics is not just a leptoquark, but supersymmetry with R-parity violation, the situation becomes much more complicated, — as is to be expected when the particle spectrum is augmented by twenty-eight new particles¹⁰ and a host of new interactions. On the negative side, the R-parity-violating squarks, which resemble leptoquarks, would have competing decay channels, weakening the resonance signals, and we demonstrate that there are indeed parts of the parameter space where such signals are no longer viable.

Supersymmetry, however, provides new detection channels, whether R-parity is conserved or not. Keeping in mind the part of the parameter space where leptoquark-like resonances would go undetected, we note that here new signals can arise from sparticle cascade decays, originating from a squark or a gluino. These cascades generally end in the lightest supersymmetric particle, which can decay to jets plus a charged lepton (or jets plus a neutrino, i.e. MET) when R-parity is violated. Accordingly, we focus on the final state with a dilepton and multiple jets (arising in the cascade decays) which is the analogue, in our case, of the jets + missing energy channel known to be the most promising of supersymmetry signals when R-parity is conserved. We demonstrate that this channel would show a large excess over the Standard Model background, both in the case when the gluino decays into squarks and when the squarks decay into gluinos. This will happen irrespective of whether a resonance can be seen or not.

In case a resonance is not seen, and we observe only the dilepton + jets signal, it may be argued, even if for the sake of argument alone, that some simple extensions of the Standard Model could also, perhaps, be tailored to produce this signal. However, supersymmetry provides another characteristic signal, which is enhanced if R-parity is violated, and this is the appearance of pairs, triads or even quartets of like-sign leptons in cascade decays of sparticles. Such signals have little

¹⁰thirty-one if there are right-handed neutrinos.

or no Standard Model background. While same-sign lepton pairs appear even in supersymmetric models where R-parity is conserved, triads and quartets can only appear if R-parity is violated. We study same-sign lepton signals, therefore, and demonstrate that for our model these combinations appear in the approximate ratio 100:10:1 respectively. The actual number will, of course, depend most crucially on the masses of the squarks and the gluino, and will, therefore, depend on the point in the supersymmetric parameter space. We explore this parameter space and find out the limits to which same-sign lepton pairs, triads and quartets can be seen. Within these limits, one should expect the resonance or dilepton + jets signals to be supplemented by the observation of such same-sign leptons. We also show that the last-mentioned category of signals could make their appearance even at the 7 TeV run of the LHC, in the most favourable part of the parameter space.

R-parity violation is admittedly not the most popular supersymmetric option, probably because it causes the lightest supersymmetric particle to decay and hence has no explanation for dark matter. However, we demonstrate in this work that it can not only correlate some of the present and projected low-energy data comprehensively, but it can also predict rather spectacular signals at the LHC — even, perhaps, in the early runs. If some such signals, e.g. same-sign triads, are actually observed, it would then be really necessary to consider the R-parity-violating version of supersymmetry in all seriousness, at the cost of leaving the dark matter problem completely open to speculation. This is an option which must be left to the future to decide, when the LHC data become available.

Acknowledgments: The authors acknowledge discussions with M. Guchait and G. Majumdar, both of the CMS Collaboration. BB would like to thank the Saha Institute of Nuclear Physics, Kolkata, for hospitality while some of the work was being done. GB would like to thank the Department of Theoretical Physics, Tata Institute of Fundamental Research, Mumbai, for an Adjunct Faculty position and for hospitality during a major part of this work.

References

- [1] For comprehensive reviews, see G. Altarelli, CERN preprint CERN-PH-TH/2008-085 (2008) [arXiv:0805.1992] and CERN preprint CERN-PH-TH/2010-249 (2010) [arXiv:1010.5637].
- [2] This is nicely discussed by C. Quigg, Fermilab preprint FERMILB-PUB-09/2307 (2009) [arXiv:0905.3187].
- [3] G. R. Farrar and P. Fayet, Phys. Lett. B **76**, 575 (1978); S. Weinberg, Phys. Rev. D **26**, 287 (1982); N. Sakai and T. Yanagida, Nucl. Phys. B **197**, 533 (1982); C. S. Aulakh and R. N. Mohapatra, Phys. Lett. B **119**, 136 (1982).
- [4] L. E. Ibanez and G. G. Ross, Phys. Lett. B **260**, 291 (1991); Nucl. Phys. B **368**, 3 (1992).
- [5] G. Bhattacharyya, K. B. Chatterjee and S. Nandi, Nucl. Phys. B **831**, 344 (2010).

- [6] D. K. Ghosh, R. M. Godbole and S. Raychaudhuri, TIFR preprint TIFR-TH-99-12 (1999) [hep-ph/9904233]; S. P. Das, A. Datta and S. Poddar, Phys. Rev. D **73**, 075014 (2006); V. M. Abazov *et al.* [D0 Collaboration], Phys. Lett. B **638**, 441 (2006); A. Datta and S. Poddar, Phys. Rev. D **75**, 075013 (2007); A. Datta and S. Poddar, Phys. Rev. D **79**, 075021 (2009); J. M. Butterworth *et al.*, Phys. Rev. Lett. **103**, 241803 (2009); N. Desai and B. Mukhopadhyaya, JHEP **1010**, 060 (2010); K. Ghosh, S. Mukhopadhyay and B. Mukhopadhyaya, JHEP **1010**, 096 (2010); S. L. Chen *et al.*, [arXiv:1011.2214] (2010).
- [7] K. Nakamura *et al.* (Particle Data Group), J. Phys. G **37**, 075021 (2010) [<http://pdg.lbl.gov>].
- [8] M. Bona *et al.*, [arXiv:0709.0451 (hep-ex)].
- [9] For reviews see, G. Bhattacharyya, Nucl. Phys. Proc. Suppl. **52A**, 83 (1997); G. Bhattacharyya, [arXiv:hep-ph/9709395]; H. K. Dreiner, [arXiv:hep-ph/9707435]; M. Chemtob, Prog. Part. Nucl. Phys. **54**, 71 (2005); R. Barbier *et al.*, Phys. Rept. **420**, 1 (2005).
- [10] For a recent update on single RPV couplings, see Y. Kao and T. Takeuchi, [arXiv:0910.4980 (hep-ph)].
- [11] G. Bhattacharyya and D. Choudhury, Mod. Phys. Lett. A **10**, 1699 (1995).
- [12] G. Bhattacharyya, H. V. Klapdor-Kleingrothaus and H. Pas, Phys. Lett. B **463**, 77 (1999); S. Rakshit, G. Bhattacharyya and A. Raychaudhuri, Phys. Rev. D **59**, 091701 (1999); A. Abada, G. Bhattacharyya and M. Losada, Phys. Rev. D **66**, 071701 (2002). This is only a partial list. See [9] for other references on neutrino mass generation by RPV couplings.
- [13] P. Dey *et al.*, JHEP **0812**, 100 (2008).
- [14] S. Nandi and J. P. Saha, Phys. Rev. D **74**, 095007 (2006).
- [15] A. Kundu and S. Nandi, Phys. Rev. D **78**, 015009 (2008); A possible contribution from λ' product couplings has also been mentioned in A. G. Akeroyd and S. Recksiegel, Phys. Lett. B **554**, 38 (2003).
- [16] For a review of all constraints on f_{D_s} , see J. L. Rosner and S. Stone, [arXiv:1002.1655 (hep-ex)], and references therein.
- [17] B. I. Eisenstein *et al.* [CLEO Collaboration], Phys. Rev. D **78**, 052003 (2008).
- [18] K. Abe *et al.* [Belle Collaboration], Phys. Rev. Lett. **100**, 241801 (2008).
- [19] P. Naik *et al.* [CLEO Collaboration], Phys. Rev. D **80**, 112004 (2009).
- [20] B. A. Dobrescu and A. S. Kronfeld, Phys. Rev. Lett. **100**, 241802 (2008); R. Benbrik and C. H. Chen, Phys. Lett. B **672**, 172 (2009); I. Doršner *et al.*, [arXiv:0906.5585 (hep-ph)].
- [21] F. Jegerlehner and A. Nyffeler, Phys. Rept. **477**, 1 (2009). For a recent update, see J. Prades, [arXiv:0909.2546 (hep-ph)].

- [22] H. Baer, V. D. Barger, D. Karatas and X. Tata, Phys. Rev. D **36**, 96 (1987) ; H. Baer, X. Tata and J. Woodside, Phys. Rev. D **41**, 906 (1990); R. Barbieri, F. Caravaglios, M. Frigeni and M. L. Mangano, Nucl. Phys. B **367**, 28 (1991); R. M. Barnett, J. F. Gunion and H. E. Haber, Phys. Lett. B **315**, 349 (1993); H. K. Dreiner, M. Guchait and D. P. Roy, Phys. Rev. D **49**, 3270 (1994).
- [23] For a recent review, see, for example, N. Öztürk, for the ATLAS and CMS Collaborations, [arXiv:0910.2964 (hep-ph)].
- [24] B. Bhattacharjee *et al*, Phys. Rev. D **81**, 035021 (2010).
- [25] V. D. Barger, G. F. Giudice and T. Han, Phys. Rev. D **40**, 2987 (1989).
- [26] G. Tonelli (CMS Collaboration), *private communication*.
- [27] B. Dion *et al.*, Eur. Phys. J. C **2**, 497 (1998); O. J. P. Éboli, R. Z. Funchal and T. L. Lungov, Phys. Rev. D **57**, 1715 (1998); A. Belyaev *et al*, Phys. Rev. D **59**, 075007 (1999); S. Abdullin and F. Charles, Phys. Lett. B **464**, 223 (1999); M. Kramer *et al.*, Phys. Rev. D **71**, 057503 (2005); P. Fileviez Perez *et al.*, Nucl. Phys. B **819**, 139 (2009); V. M. Abazov *et al.* [D0 Collaboration], Phys. Lett. B **693**, 95 (2010).
- [28] B. Mukhopadhyaya and S. Mukhopadhyay, Phys. Rev. D **82**, 031501 (2010).
- [29] T. Sjöstrand, S. Mrenna and P. Z. Skands, JHEP **0605**, 026 (2006).
- [30] A. Djouadi, J.L. Kneur and G. Moultaka, CERN preprint CERN-TH/2002-32 (2002) [hep-ph/0211331].
- [31] S. Cucciarelli (CMS Collaboration), Nuclear Physics B (Proc. Suppl.) **120**, 190 (2003); M. Lehmacher (ATLAS Collaboration) [arXiv:0809.4896 (hep-ex)].
- [32] E. Cremmer *et al.*, Phys. Lett. B **79**, 231 (1978); Nucl. Phys. B **147**, 105 (1979); R. Barbieri, S. Ferrara, and C. A. Savoy, Phys. Lett. B **119**, 343 (1982); A. H. Chamseddine, R. L. Arnowitt, and P. Nath, Phys. Rev. Lett. **49**, 970 (1982); L. J. Hall, J. D. Lykken, and S. Weinberg, Phys. Rev. D **27**, 2359 (1983); P. Nath, R. L. Arnowitt, and A. H. Chamseddine, Nucl. Phys. B **227**, 121 (1983); N. Ohta, Prog. Theor. Phys. **70**, 542 (1983). For more recent analyses, see, for example, O. Buchmüller *et. al*, Eur. Phys. J. C **71**, 1583 (2011) and references therein.
- [33] B. C. Allanach, A. Dedes and H. K. Dreiner, Phys. Rev. D **69**, 115002 (2004); [Erratum-ibid. D **72**, 079902 (2005)].
- [34] H. Baer, A. Lessa and H. Summy, Phys. Lett. B **674**, 49 (2009); H. Baer, V. Barger, A. Lessa and X. Tata, JHEP **0909**, 063 (2009); J. Edsjo, E. Lundstrom, S. Rydbeck and J. Sjölin, JHEP **1003**, 054 (2010).